Journal of Multidisciplinary Modeling and Optimization

Volume:3

Issue: 1

E-ISSN: 2645-923X

http://dergipark.gov.tr/jmmo

TABLE OF CONTENTS

Journal of Multidisciplinary Modeling and Optimization 3(1) (2020), 1-11.

Parameterized Three-Term Conjugate Gradient Method

Khalil K. ABBO [1] and Nehal H. HAMEED[2]

[1]Department of Mathematics,
Telafer University, Mosul, Iraq
kh_196538@yahoo.com

[2]Department of Mathematics,
Mosul University, Mosul, Iraq
Nehalh926@gmail.com

Received: 28.12.2019, Accepted: 21.08.2020, Published: 17.09.2020

Abstract — *In this paper a new parameterized three-term conjugate gradient algorithm is suggested, the descent property and global convergence are proved for the new suggested method. Numerical experiments are employed to demonstrate the efficiency of the algorithm for solving large scale benchmark test problems, particularly in comparison with the existent state of the art algorithms available in the literature..*

Keywords: Three-term conjugate gradient, Global convergence, Large scale benchmark test.
Mathematics Subject Classification: 65K10, 90C30, 90C26.

1 Introduction

Consider the non-linear unconstrained optimization problem

$$\min\{f(x): x \in R^n\} \tag{1.1}$$

where $f: R^n \to R$ is continuously differentiable function and bounded from below. There are many different methods for solving the problem (1.1) see [8, 10, 12, 15]. We are interested in conjugate gradient (CG) methods, which have low memory requirements and strong local and global convergence properties [2,13].

For solving the problem (1.1), we consider the CG method, which starts from an initial point $x_1 \in R^n$ and generates a sequence $\{x_k\} \subset R^n$ as follows

$$x_{k+1} = x_k + \alpha_k d_k \tag{1.2}$$

where $\alpha_k > 0$ is a step size, received from the line search, and directions d_k are given [2,17] by, $d_1 = -g_1$ and

$$d_{k+1} = -g_{k+1} + \beta_k s_k \tag{1.3}$$

Cite as: *K. K. Abbo and N. H. Hameed, Parameterized Three-Term Conjugate Gradient Method, Journal of Multidisciplinary Modeling and Optimization 3(1) (2020), 1-11.*

In the equation (1.3) $g_k = \nabla f(x_k)$, $s_k = x_{k+1} - x_k$ and β_k is the conjugate gradient parameter. Various choices of the scalar β_k exist which give different performance on non-quadratic functions, yet they are equivalent for quadratic functions. In order to choose the parameter β_k for the method in present paper, we mention the following choices:

$\beta^{FR} = \dfrac{g_{k+1}^T g_{k+1}}{g_k^T g_k}$ Fletcher-Reeves [9]

$\beta^{HS} = \dfrac{g_{k+1}^T y_k}{d_k^T y_k}$ Hestenses-Stiefel [11]

$\beta^{PR} = \dfrac{g_{k+1}^T y_k}{g_k^T g_k}$ Polak-Ribiere[16]

$\beta^{LS} = -\dfrac{y_k^T g_{k+1}}{g_k^T d_k}$ Liu-Story[14]

$\beta^{DX} = -\dfrac{g_{k+1}^T g_{k+1}}{g_k^T d_k}$ Dixon [6]

where $y_k = g_{k+1} - g_k$.

Zhang (Zhang et al., 2006) have proposed the three – term FR, PR and HS conjugate gradient methods. Their methods always satisfy the descent condition $d_k^T g_k < 0$ or sufficient descent condition $d_k^T g_k = -c\|g_k\|$, where c positive constant, these methods have the following search directions:

1- FR three - term is

$$d_{k+1} = -g_{k+1} + \beta^{FR} d_k - \theta_k^{(1)} g_{k+1}, \quad \theta_k^{(1)} = \frac{d_k^T g_{k+1}}{g_k^T g_k} \tag{1.4}$$

2- PR three - term is

$$d_{k+1} = -g_{k+1} + \beta^{PR} d_k - \theta_k^{(2)} y_k, \quad \theta_k^{(2)} = \frac{g_{k+1}^T d_k}{g_k^T g_k} \tag{1.5}$$

3-HS three - term is

$$d_{k+1} = -g_{k+1} + \beta^{HS} d_k - \theta_k^{(3)} y_k, \quad \theta_k^{(3)} = \frac{g_{k+1}^T d_k}{d_k^T y_k} \tag{1.5}$$

we note that these methods always satisfy:

$$d_k^T g_k = -c\|g_k\|^2 < 0 \qquad \forall k \tag{1.6}$$

which implies the sufficient descent condition with $c = 1$.

The standard Wolfe (WC) line search conditions are frequently used in the conjugate gradient methods, these conditions are given in [18]

$$f(x_k+\alpha_k d_k) \le f(x_k)+\rho\alpha_k g_k^T d_k \tag{1.7}$$

$$g_{k+1}^T d_k \ge \sigma\, g_k^T d_k \tag{1.8}$$

where d_k is descent direction ie $g_k^T d_k < 0$ and $0<\rho<\sigma<1$. Strong Wolfe (SWC) conditions consist of (1.7) and the next stronger version of (1.8)

$$\left| g_{k+1}^T d_k \right| \le -\sigma\, g_k^T d_k \tag{1.9}$$

2 A New Modified Three–Term Conjugate Gradient (KN2).

In this section we develop a new three term conjugate gradient method (KN2), our idea is based on the following well-known Zhang's three terms CG-method:

$$x_{k+1} = x_k + \alpha_k d_k \tag{2.1}$$

$$d_{k+1} = \begin{cases} -g_1, & if\ \ k=0, \\ -g_{k+1}+\beta_k^{DL} d_k - \xi_k (\mathrm{y}_k - \mathrm{t}\mathrm{s}_k), & \text{if } \ \mathrm{k} \ge 1, \end{cases} \tag{2.2}$$

where

$$\beta_k^{DL} = \frac{g_{k+1}^T (y_k - t s_k)}{d_k^T y_k} \quad ,t \ge 0 \quad \text{ and } \xi_k = \frac{g_{k+1}^T d_k}{d_k^T y_k} \tag{2.3}$$

If exact line search is used then $g_{k+1}^T d_k = 0$, therefore the method (2.2) reduces to the classical Liu and Story [14] conjugate gradient method, furthermore if the objective function is convex quadratic and line search is exact then (2.2) reduces to the DX method[6]. The method defined in (2.2)-(2.3) has some disadvantages for example, the value of t is unknown, which is crucial for β_K^{DL}.

To overcome to this disadvantage, we suggest the following search direction:

$$d_{k+1} = -g_{k+1} + \beta_k^{FR} s_k - \xi(\mathrm{y_k} - \mathrm{s_k}) \tag{2.4}$$

To find the value of ξ, we multiply (2.4) by y_k^T we get:

$$d_{k+1}^T \mathrm{y_k} = -g_{k+1}^T \mathrm{y_k} + \beta_k^{FR} s_k^T \mathrm{y_k} - \xi(\mathrm{y_k}-\mathrm{s_k})^T \mathrm{y_k} = 0$$

$$= -g_{k+1}^T \mathrm{y_k} + \beta_k^{FR} s_k^T \mathrm{y_k} - \xi\, y_k^T \mathrm{y_k} + \xi\, s_k^T \mathrm{y_k} = 0$$

$$= -g_{k+1}^T \mathrm{y_k} + \beta_k^{FR} s_k^T \mathrm{y_k} - \xi(y_k^T \mathrm{y_k} - s_k^T \mathrm{y_k}) = 0$$

then

$$\xi = \frac{\beta^{FR} s_k^T \mathrm{y_k} - g_{k+1}^T \mathrm{y_k}}{y_k^T \mathrm{y_k} - y_k^T \mathrm{s_k}} \tag{2.5}$$

hence we obtain the following new(KN2) search direction:

$$d_{k+1} = -g_{k+1} + \beta_k^{FR} s_k - \frac{\beta^{FR} s_k^T \mathrm{y_k} - g_{k+1}^T \mathrm{y_k}}{y_k^T \mathrm{y_k} - y_k^T \mathrm{s_k}} (\mathrm{y_k} - \mathrm{s_k}) \tag{2.6}$$

Some Remarks on The New(KN2) Method:

1- If the line search is exact i.e. $g_{K+1}^{\mathrm{T}} \mathrm{s_k} = 0$,then the search direction in (2.6) reduces to the following one .

$$d_{k+1} = -g_{k+1} + \beta_k^{FR} s_k + \frac{\beta^{FR} s_k^T g_{\mathrm{k}} + g_{k+1}^T \mathrm{y_k}}{y_k^T \mathrm{y_k} + s_k^T g_{\mathrm{k}}} (\mathrm{y_k} - \mathrm{s_k}) \tag{2.7}$$

If the objective function is convex quadratic and line search is exact , $g_{\mathrm{k+1}}^{\mathrm{T}} \mathrm{g_k} = 0$ and $s_{\mathrm{k}}^{\mathrm{T}} \mathrm{g_{k+1}} = 0$, then

$$\begin{aligned}
y_{\mathrm{k}}^{\mathrm{T}} \mathrm{y_k} &= \mathrm{y_k^T}(g_{k+1} - g_k) \\
&= \mathrm{y_k^T} g_{k+1} - y_k^T g_k \\
&= (g_{k+1} - \mathrm{g_k})^T g_{k+1} - (g_{k+1} - g_k)^T g_k \\
&= g_{k+1}^T \mathrm{g_{k+1}} - g_k^T g_{k+1} - g_{k+1}^T g_k + g_k^T g_k \\
&= g_{k+1}^T g_{k+1} + g_k^T g_k
\end{aligned}$$

then the search direction defined in (2.6) reduces to the following

$$d_{k+1} = -g_{k+1} + \beta_k^{FR} s_k + \frac{\beta^{FR} s_k^T g_{\mathrm{k}} + g_{k+1}^T g_{\mathrm{k+1}}}{g_{k+1}^T g_{\mathrm{k+1}} + g_k^T g_{\mathrm{k}} + s_k^T g_{\mathrm{k}}} (\mathrm{y_k} - \mathrm{s_k}) \tag{2.8}$$

Note that we denote the search directions defined in (2.7) and (2.8) as KN2-1 and KN2-2, respectively.

Now we give the corresponding algorithms.

Algorithm (KN2):

Step1. Initialization: Select the initial point $x_1 \in \mathrm{R}^{\mathrm{n}}$, $\varepsilon > 0$, and select the parameters $0 < \rho < \sigma < 1$. Set $k = 1$. Compute f_k, g_k. Set

$d_k = -g_k$ and set $\alpha_k = \dfrac{1}{\|g_k\|}$.

Step2. Test for continuation of iterations. If $\|g_k\| \le \varepsilon$, then stop

Step3. Line search. Compute $\alpha_k > 0$ satisfying the standard Wolfe conditions (1.7) and(1.8) or strong Wolfe (1.7) and (1.9)

and update the variables $x_{k+1} = x_k + \alpha_k d_k$, compute

f_{k+1}, g_{k+1} , $y_k = g_{k+1} - g_k$ and $s_k = x_{k+1} - x_k$

Step4. Set $\beta_k = \beta_k^{FR}$ and compute ξ . If $y_k^T y_k - y_k^T s_k = 0$, then set $\xi = 0$ else set ξ as in (2.5).

Step5. If the restart criterion is satisfied, then set

$d_{k+1} = -g_{k+1}$ else compute d_{k+1} from (2.6).

Step6. Calculate the initial guess $\alpha_{k+1} = \alpha_k \|d_k\| / \|d_{k+1}\|$

Step7. Set $k = k+1$ go to **step 2**.

To prove the sufficient descent property to the algorithm KN2 we need the following theorem.

Theorem 2.1 [1]. If an α_k is calculated which satisfies strong Wolfe conditions (1.7) and (1.9) with $\sigma \in (0, \frac{1}{2}]$ for all k and $(g_k \ne 0)$, then the descent property for the Fletcher-Reeves method holds for all k.

In the following theorem we will show that the search directions generated by equation (2.6) are descent directions.

Theorem 2.2. Consider the search directions defined by the equation (2.6). Let the step-size α_k satisfies the strong Wolfe conditions (1.7), (1.9) and assume that the condition $y_k^T g_{k+1} \le \beta_{k+1}^{FR} s_k^T y_k$ hold then

$d_{k+1}^T g_{k+1} \le -c\|g_{k+1}\|$

Proof: If k=0, then $d_1 = -g_1$ and we get $d_1^T g_1 = -\|g_1\|^2 < 0$ where $c = -1$

Suppose $d_k^T g_k \le -c\|g_1\|^2$, to prove for k+1 consider the search direction defined in (2.6)

$$d_{k+1} = -g_{k+1} + \beta^{FR}\ s_k - \frac{\beta_{k+1}^{FR} s_k^T y_k - g_{k+1}^T y_k}{y_k^T y_k - y_k^T s_k}(y_k - s_k)$$

We multiply by g_{k+1}^{T} then,

$$g_{k+1}^T d_{k+1} = -g_{k+1}^T g_{k+1} + \beta^{FR}\ g_{k+1}^T s_k - \frac{\beta_{k+1}^{FR} s_k^T y_k - g_{k+1}^T y_k}{y_k^T y_k - y_k^T s_k} g_{k+1}^T (y_k - s_k)$$

$$\leq -\|g_{k+1}\|^2 + \beta^{FR}\ g_{k+1}^T s_k - \frac{\beta_{k+1}^{FR} s_k^T y_k - g_{k+1}^T y_k}{y_k^T y_k - y_k^T s_k} g_{k+1}^T (y_k - s_k)$$

$$= -\|g_{k+1}\|^2 + \beta^{FR}\ g_{k+1}^T s_k - \frac{\beta_{k+1}^{FR} s_k^T y_k}{y_k^T y_k - y_k^T s_k} g_{k+1}^T (y_k - s_k) + \frac{g_{k+1}^T y_k}{y_k^T y_k - y_k^T s_k} g_{k+1}^T (y_k - s_k)$$

Since $y_k^T g_{k+1} \leq \beta_{k+1}^{FR} s_k^T y_k$ therefor $g_{k+1}^T d_{k+1} \leq -g_{k+1}^T g_{k+1} + \beta_{k+1}^{FR}\ g_{k+1}^T s_k$ which is Fletcher-Reeves search direction, therefor by theorem (2.1), $g_{k+1}^T d_{k+1} \leq -(1-\sigma^k)\|g_{k+1}\|^2$ where $\sigma \leq 1/2$.

On the other hand the search directions generated by the equation (2.6) are conjugate directions for all k.

3 Convergence Analysis

At first, we give the following basic assumption on the objective function Assumption 2.1

i-The level $S = \{x \in R^n \mid f(x) \leq f(x_1)\}$ is bounded, where x_1 is the starting point then there exists a constant $\gamma_1 > 0$. such that:

$$\|x\| \leq \gamma_1 \qquad \textit{for all } x \in S \tag{3.1}$$

ii- In some neighborhood N of continuously differentiable and its gradient is Lipchitz continuous with Lipchitz constant $L > 0$, .i.e

$$\|g(u) - g(w)\| \leq L\|u-w\| \qquad \forall\ u,w \in N \tag{3.2}$$

Assumption (2.1.ii) implies that there exists a positive constant γ_2 such that

$$\|g(x)\| \leq \gamma_2 \qquad \forall\ x \in S \tag{3.3}$$

Proposition 3.1. Suppose that Assumption (2.1) is satisfied, and consider any conjugate gradient method, where d_k is descent direction and α_k is obtained by the Wolfe conditions. If $\sum_{k=1}^{\infty} \frac{1}{\|d_k\|^2} = \infty$ then $\lim_{k \to \infty} \inf \|g_k\| = 0$ for prove see [10].

In the rest of this section, we assume $g_k \neq 0$ *for all* k, otherwise a stationary point has been found. Under Assumption(2.1) , and Zoutendijk condition we can use the following theorem to prove the global convergence of the (KN2).

Theorem 3.1. Suppose that Assumption (2.1) is satisfied. Consider the KN2 method where d_k is descent direction and α_k satisfies Wolfe(standard or strong) conditions then $\lim_{k \to \infty} \inf \left\| g_k \right\| = 0$.

Proof: From equations (2.6), (3.1), (3.2) and (3.3)we have

$$\begin{aligned}
\left\| d_{k+1} \right\| &= \left\| -g_{k+1} + \beta^{FR} s_k - \frac{\beta^{FR} s_k^T y_k - g_{k+1}^T y_k}{y_k^T y_k - s_k^T y_k} (y_k - s_k \right\| \\
&\leq \left\| g_{k+1} \right\| + \left| \beta^{FR} \right| \left\| s_k \right\| + \left| \frac{\beta^{FR} s_k^T y_k - g_{k+1}^T y_k}{y_k^T y_k - s_k^T y_k} \right| (\left\| y_k - s_k \right\|) \\
&\leq \left\| g_{k+1} \right\| + \left| \beta^{FR} \right| \left\| s_k \right\| + \left| \beta^{FR} \right| \frac{\left\| g_{k+1} \right\| \left\| s_k \right\| L}{2} (L+1) \left\| s_k \right\|) \\
&\leq \gamma_2 + \gamma_1 + \frac{\gamma_2 \gamma_1 L}{2} (L+1) \gamma_1 = \frac{2(\gamma_2 + \gamma_1) + (L+1) \gamma_2 \gamma_1 L}{2}
\end{aligned}$$

Let $\gamma = \max(\gamma_2, \gamma_1)$ therefore

$$\sum_{k=1}^{\infty} \left\| d_{k+1} \right\| \leq \sum_{k=1}^{\infty} \frac{4\gamma + (L+1)\gamma^2 L}{2}$$

$$\sum_{k=1}^{\infty} \frac{1}{\left\| d_{k+1} \right\|} \geq \sum_{k=1}^{\infty} \frac{2}{4\gamma + (L+1)\gamma^2 L} = \infty$$

Hence by proposition(3.1) $\lim_{k \to \infty} \inf \left\| g_k \right\| = 0$

4 Numerical Results

This section presents the performance of FORTRAN implementation of our new three-terms conjugate gradient (KN2) algorithm on a set of unconstrained optimization test problems. We selected a number of 72 large-scale unconstrained optimization test problems in extended or generalized form presented in [3]. For each test function, we have considered numerical experiments with the number of variables increasing as n=100, …,1000. The algorithms uses the Wolfe line search conditions (1.7)and (1.8)with cubic interpolation, $\rho = 0.0001$ *and* $\sigma = 0.9$ and the same stopping criterion $\left\| g_k \right\|_2 \leq 10^{-6}$, where $\left\| . \right\|_2$ is the Euclidean norm.

The algorithms we compare in these numerical experiments find the local solutions. Therefore, the comparisons of algorithms are given in the following context. Let f_i^{ALG1} and f_i^{ALG2} be the optimal value found by ALG1 and ALG2 for problem i=1,…,720, respectively. We say that in the particular problem i , the performance of ALG1 was better than the performance of AlG2 if:

$$\left\| f_i^{ALG1} - f_i^{ALG2} \right\| < 10^{-3}$$

and number of iterations (iter), or the number of function-gradient evaluations (fg), or the CPU time corresponding to ALG2 respectively. We have compared our algorithm versus to the following algorithms:

1-Three term Fletcher-Revees (1.4).

2-Three term Hestenes-Stiefel (1.5).

In all these algorithms, the initial step size is $\alpha_1 = 1/\|g_1\|$ and initial guess for other iterations i.e. ($k > 1$) is $\alpha_k = \alpha_{k+1}(\|d_{k+1}\|/\|d_k\|)$.

The codes are written in double precision FORTRAN (2000) and compiled with F77 default compiler setting. This code originally written by Andrei and we modified it.

Figures 1, 2 and 3 show performance of these methods for solving 72 unconstrained optimization test problems for dimensions n=100,..,1000, relative to the iterations (iter), function–gradient evaluations (fg) and CPU time, which are evaluated using the profile of Dolan and More [7]. That is, for each method, we plot the fraction p of problems for which the method is within a factor τ of the best (iter) or (fg) or CPU time. The left side of the figure gives the percentage of the test problems for which a method is the fastest, the right side gives the percentage of the test problems that are successfully solved by each of the methods. The top curve is the method that solved the most problems in a (iter, fg, time) that was within a factor τ of the best (iter, fg, time).

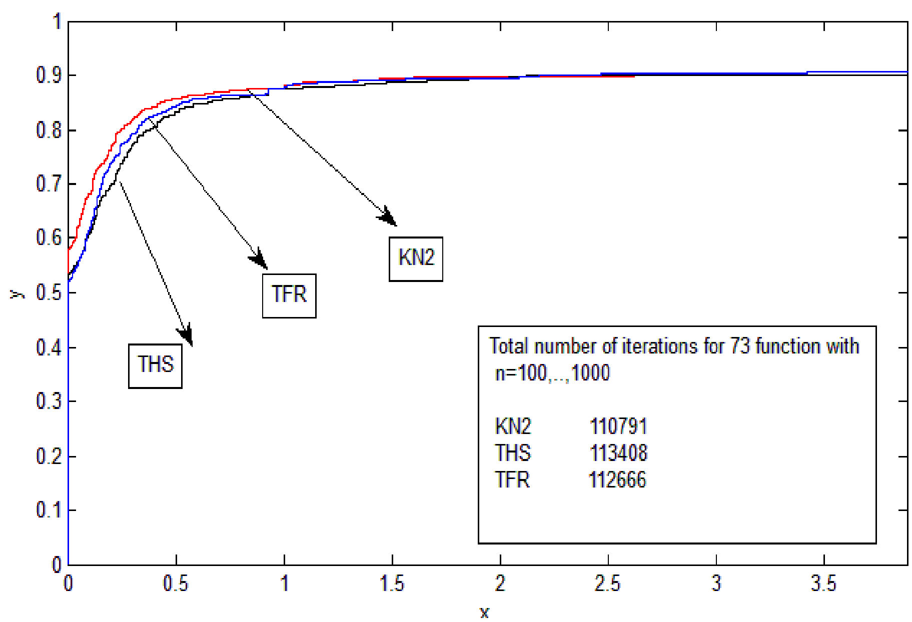

Figure 1: Performance Based on Number of Iterations

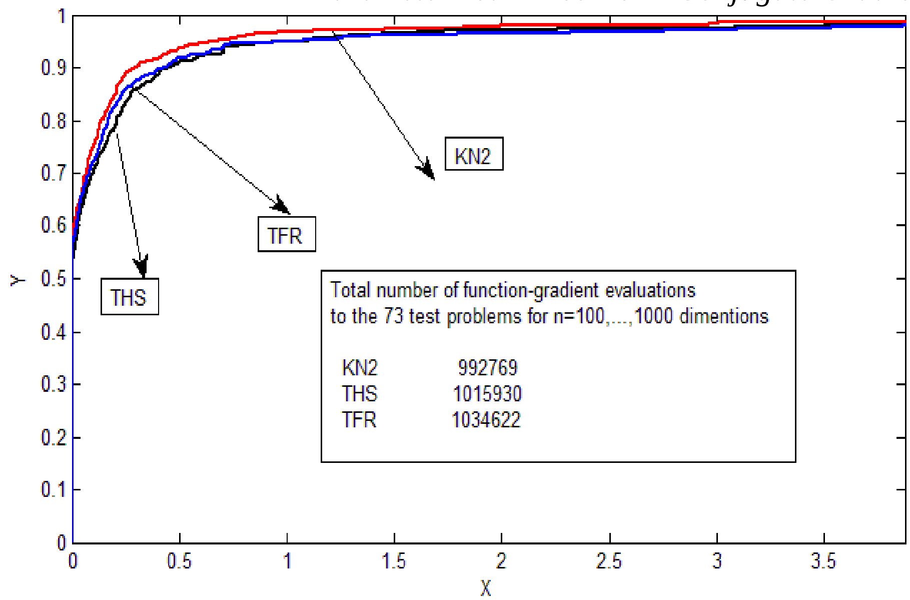

Figure 2: Performance Based on Number of Function-Gradient Evaluations

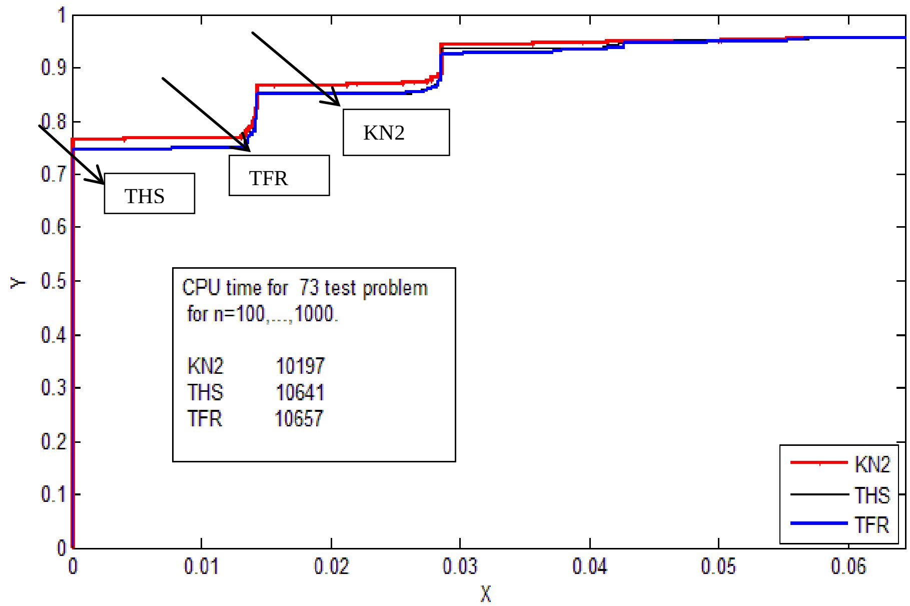

Figure 3: Performance Based on CPU Time in Seconds

Acknowledgment

The authors declare that this work is completely private effort and it has not been supported by any governmental, financial, educational or otherwise establishment.

Conflict of Interest Declaration

The authors declare that there is no conflict of interest statement.

Ethics Committee Approval and Informed Consent

The authors declare that declare that that there is no ethics committee approval and/or informed consent statement.

References

[1] M. Al-Baali, Descent property and global convergence of the Fletcher Reeves method with inexact line search, IMA J. Numer. Anal., 5(1) 1985, 121-124.

[2] N. Andrei, New Hybrid Conjugate Gradient Algorithms for Unconstrained Optimization . In: Floudas C., Pardalos P. (eds) Encyclopedia of Optimization, Springer, Boston, 2008, 2560-2571.

[3] N. Andrei, An unconstrained optimization test functions collection, Adv. Model. Optim, 10(1) 2008, 147-161.

[4] I. Bongartz, A. Conn, N. Gould and P. Toint, Constrained and unconstrained testing environment, J. Optim. Theory Appl., 21(1) 1993, 123-160.

[5] Y. Dai, Y. Yuan, A nonlinear conjugate gradient method with a strong global convergence property, SIAM J. Optimiz., 10(1) 1999, 177-182.

[6] L. C.W. Dixon, Nonlinear optimization: A survey of the state of the art, Hatfield Polytechnic. Numerical Optimization Centre, 1973.

[7] D. Dolan, J. Mor´e, Benchmarking optimization software with performance profiles, Math. Program., 91(2) 2002, 201-213.

[8] K. Edwin, H. Stanilow, An introduction to optimization, Second Edition, Wiley and Sons, 2001.

[9] R. Fletcher, C. M. Reeves, Function minimization by Conjugate gradients, Comput. J., 7(2) 1964, 149-154.

[10] W. Hager, H. Zhang, A survey of nonlinear conjugate gradient methods, Pac. J. Optim., 2(1), 2006, 35-58.

[11] M. Hestenes, E. Stiefel, Methods of conjugate gradients for solving linear systems, J. Res. Nat. Bur. Stand., 49(1) 1952.

[12] K. K. Abbo, L. A. Abdulwahid, Generalized Dai-Yuan non-linear conjugate gradient method for unconstrained optimization,

Int. J. Sci. Math. Educ., 8(6) 2017, 17993-17999,

[13] X. Li, X. Zhao, A hybrid conjugate gradient method for optimization problems, Nat. Sci., 3(1) 2011, 85.

[14] Y. Liu, C. Storey, Efficient generalized conjugate gradient algorithms, part 1: theory, J. Optimiz. Theory App., 69(1) 1991, 129-137.

[15] J. Nocedal, J. Wright, Numerical Optimization, Springer Series in Operations Research, Springer Verlag, New York, 2006.

[16] E. Polak and G. Ribiere, Note sur la convergence de m´ethodes de directions conjugu´ees, Rev. Fr. Inform. Rech. O., 3(16) 1969, 35-43,

[17] S. S. Djordjevi, New hybrid conjugate gradient method as a convex combination of FR and PRP Methods. Filomat, 30(11) 2016, 3083-3100,

[18] P. Wolfe, Convergence conditions for ascent methods, SIAM Rev., 11(2) 1969, 226-235,

Khalil K. Abbo, ORCID: https://orcid.org/0000-0001-5858-625X
Nehal H. Hameed, ORCID: https://orcid.org/0000-0002-4548-3091

Journal of Multidisciplinary Modeling and Optimization 3(1) (2020), 12-26.

Empirical Parametrization of COVID-19 Virus Pandemic

Aasim A. Azooz[1]

[1]Former Professor of Applied Physics,
Mosul University,Mosul, Iraq
aasimazooz1@yahoo.com

Received: 26.06.2020, Accepted: 17.08.2020, Published: 17.09.2020

Abstract — *Published global data for the infections and mortalities caused by the corona virus for the period between January-22 and June-1-2020 are used to build and test an empirical model equation that uses past trends in the data to predict near and medium future behavior of the pandemic. Extrapolation of the empirical model equation suggested for the time development of the numbers of infections and deaths is used to make approximate predictions concerning the disease leveling of the ultimate numbers of infections and deaths. Such analysis can be useful in the assessment of the particular measures adapted by each country in its efforts to hinder the spread of the virus infections.*

Keywords: COVID-19, Corona, Modeling, Pandemic modeling.
Mathematics Subject Classification: 93A30, 97M10.

1 Introduction

It is now a trivial fact that the whole world has been taken off guard as far as the COVID-19 pandemic is concerned. Furthermore, this pandemic exposed the insufficiency of the degree of readiness of most twenty first century healthcare systems round the world to handle such pandemic. The main reason for such uncoordinated handling of the situation is related to the unique combination of two intrinsic characteristics of this virus. The first is the virus ability to cause infection through the respiration inlets [1, 2, 3]. The second is the virus relatively long incubation period of about two weeks [4, 5, 6]. Such incubation period allows an infected asymptomatic individual to travel round the world several times, unknowingly transmitting the disease to whoever he comes in nearby with. These two properties played a crucial role in assisting the wide spread of infections through the utilization of the world air traffic. All this has caused the fast spread of the pandemic worldwide.

Under such desperate situation of an exponential worldwide pandemic, world countries found themselves almost helpless in taking any measures to combat the pandemic apart from imposing one degree or another social distancing measure. This was coupled with some *ad hoc* efforts to find a vaccine or treatment for the disease by the most advanced countries. In spite of all such latter efforts, the nearest projected date for an effective medical treatment or vaccine seems months away in the least [7, 8]. With world modern civilization at an almost complete halt, the only current hope and course of action so far is

Cite as: *A. A. Azooz, Empirical parametrization of COVID-19 virus pandemic, Journal of Multidisciplinary Modeling and Optimization 3(1) (2020), 12-26.*

to wait and see if nature will play some role in bringing the pandemic to a halt or a slow-down at least. The only helping hands man can give are the commitment to social distancing [9, 10, 11], and the full obedience to the rules of general hygiene.
After the initial shock wave, the major part of the world efforts in combating this pandemic has concentrated on finding medical treatments and vaccines that can help in halting the virus spread. Such effort have been going side by side with many other efforts devoted to establishing and refining statistical, mathematical and empirical modeling related to the nature and properties of this pandemic [12-20]. Such modeling plays an important role in the decision making process regarding the adaptation of the optimum strategies aiming to hinder the virus spread on one hand and minimize the resulting economic damages on the other hand.
It is the purpose of this work to suggest and test a collective empirical model that can be used in assessing the development and spread of this pandemic in the world as a whole and in any particular country. Such model can help decision makers in their evaluation of the different actions that need to be taken.

2 The Data

The data used in this work came from the world meter web site [21]. Starting on January-22-2020, the data used are update up to June-1-2020. This site is updated daily. It provides data for the numbers of infections, deaths and recoveries for all world countries and their corresponding global totals. It must be said however that the site compiles data issued by government of all countries listed. The accuracies of these data depend on each particular government openness about the matter.
Figure 1 shows a summary of the percentage daily increases in infections and deaths registered globally between Jan-22 and June-1-2020. The figure shows that at the early stage when the majority of infection took place in China, the percentage daily increases were so high reaching the value of about 35% at some stage. However, this ratio dropped to only about 2% some time by the end of February when China announced that it had the pandemic under control. At that stage, the number of infections elsewhere were small compared to those in China. This situation did not last long and soon enough Europe and the United States began to feel the burden, registering increasing numbers of infections and mortalities by the first week of March. The situation worsened with daily increases reaching 12% by the second half of March.
Social distancing which may be coupled with other still not well understood environmental conditions helped in bringing the pandemic under some kind of contagious control. This resulted in a drop in daily increased infections ratio to about 2% again after about four months from the original onset of the pandemic.

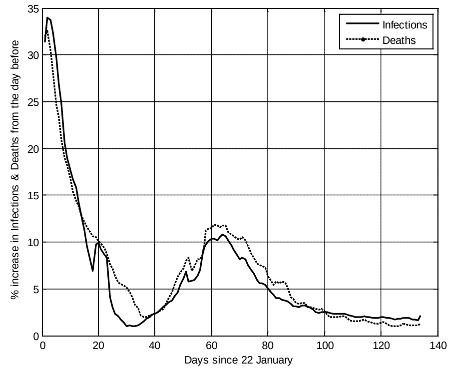

Figure 1. Percentage daily global increases of COVID-19 infections and death

3 Empirical Modelling of the Pandemic

Severe enough as it is, the current coronavirus pandemic should not deviate in its behavior from that of any other typical pandemic. Such behavior is characterized by three stages. The first is the initial onset which is usually relatively slow. The second is the fast and sharp rise in the number of infections and casualties. The third is the leveling of the number of daily infections and deaths. This chain of events are expected to take place even with the worst case scenario of no vaccine and no treatment. In such a case, and as far as COVID-19 is concerned, it has become a well-established fact that the mortality rate within those infected is few percent. This means that infections leveling must be reached even if the whole world population is to be infected at the super heavy price of several hundred million casualties. Consequently, one can safely assume the universality of the above three stages in all pandemics. The main differences between one pandemic and another are the speed by which infections increase during the second stage, and the time needed to reach the third stage. Such typical behavior can be mathematically described by a tangent hyperbolic function (***tanh***). This function is characterized by all above three properties of initial slow buildup, a following sharp rise and an ultimate saturation. Consequently, one can describe the accumulated number of infections or deaths (*N*) by an empirical equation of the form

$$N = e^{a_1 tan\,h\left[\frac{(t-a_2)}{a_3}\right]} + a_4 \qquad (1)$$

The exponentiation of the tangent hyperbolic function is introduced for enabling the equation to describe the asymmetry between the start of the rising part and the approach to leveling saturation of the data.

With t being the time in days, a_1, a_2, a_3, and a_4 are free fitting parameters to be determined by the data. These four fitting parameters carry physical significance. The parameter a_1 and a_4 form a direct measure of the total number of infections registered throughout the pandemic when leveling off takes place this number is equal to $(e^{a_1} - a_4)$. The parameter a_2 determines the amount of horizontal shift on the time axis. The third parameter a_3 governs the speed by which the pandemic is spreading. Such behavior applies to all pandemics including the COVID-19 virus.

Equation (1) is used to fit COVID-19 infection data for nineteen world countries and those for the whole world. In all cases, good convergent fits with over 95% confidence level are obtained using MATLAB nonlinear fitting facility.

Although finding a suitable empirical parametrization fitting equation for any data is regarded as one of the standard accepted scientific research tools, such parametrization usually acquires added importance if the fitted empirical equation can be extrapolated to give predictions outside the domain of the measured data. Acting within this criteria, equation (1) must not only be able to describe known registered infection data, but it should also be able to produce reasonable predictions concerning the future development of the pandemic within any country and for the world. Furthermore, it will be an added advantage if the equation is able to produce reasonable predictions on the approximate date when the pandemic will level off in any particular country. Such estimations need to be made at the earliest possible date from the pandemic onset. There is only little advantage in making predictions when the pandemic is approaching near the leveling off stage.

In order to achieve the above goals, world countries are categorized into four groups based on data available by June-1-2020. Group (I), includes countries where the pandemic has already reached or closely approached the leveling off stage. These countries include China, South Korea, Greece, and Switzerland. Group (II) category includes countries which are close to reaching the leveling off saturation of infections. Examples of such countries are Spain, Italy, France, and Turkey. Group (III) includes countries where the pandemic is still on the rise with indication of slowing down. This group includes both Russia, UK and USA. The whole world fall into this category. The forth category represents countries where infections are in the fast increasing stage. Examples are India, Chile, and Brazil.

Data for the period January-22 and June-1-2020 obtained from reference [21] for nineteen countries and the whole world within the four categories defined above are fitted to equation (1). Good fits with over 95% confidence levels are obtained using the MATLAB nonlinear fitting facility [22]. Typical examples for the four groups are presented in Figure 1. All fits are extrapolated to 300 days after the last data point on June-1-2020. Each plot in Figure 1 also shows as a black square the last data point belonging to June-1-2020 used in the fit indicating its position relative to the fit ultimate horizontal saturation which marks infections leveling off. Furthermore, the plots show the position of the curve inflection point as a black circle. This point will have an important role in the following analysis.

From mathematical point of view, the inflection point is defined as the point at which the curvature of a curve shifts from being concave upwards to concave down wards or vice versa. Mathematically, the second derivative of the curve at this point is equal to zero. Applying this condition on equation (1) and solving gives the position (X_I) of the inflection point for the general curve in equation (1) as:

$$X_I = a_3 tanh^{-1}\left[\frac{(1+a_1^2)^{1/2}-1}{a_1}\right] - a_2 \tag{2}$$

It is well known fact that the quality and robustness of any empirical fitting procedure are governed by two factors. The first is the suitability of the fitting equation in describing the fitted data. The second is the number of data points. The larger this number the better the fit. A general rule of thumb in this respect is that the number of data points should be much larger than the number of free fitting parameters within the fitted equation. It is clear from Figure 1 that equation (1) satisfies both above conditions. Fits with good qualities similar to those shown in Figure 1 are obtained for all nineteen countries plus those of world data studied.

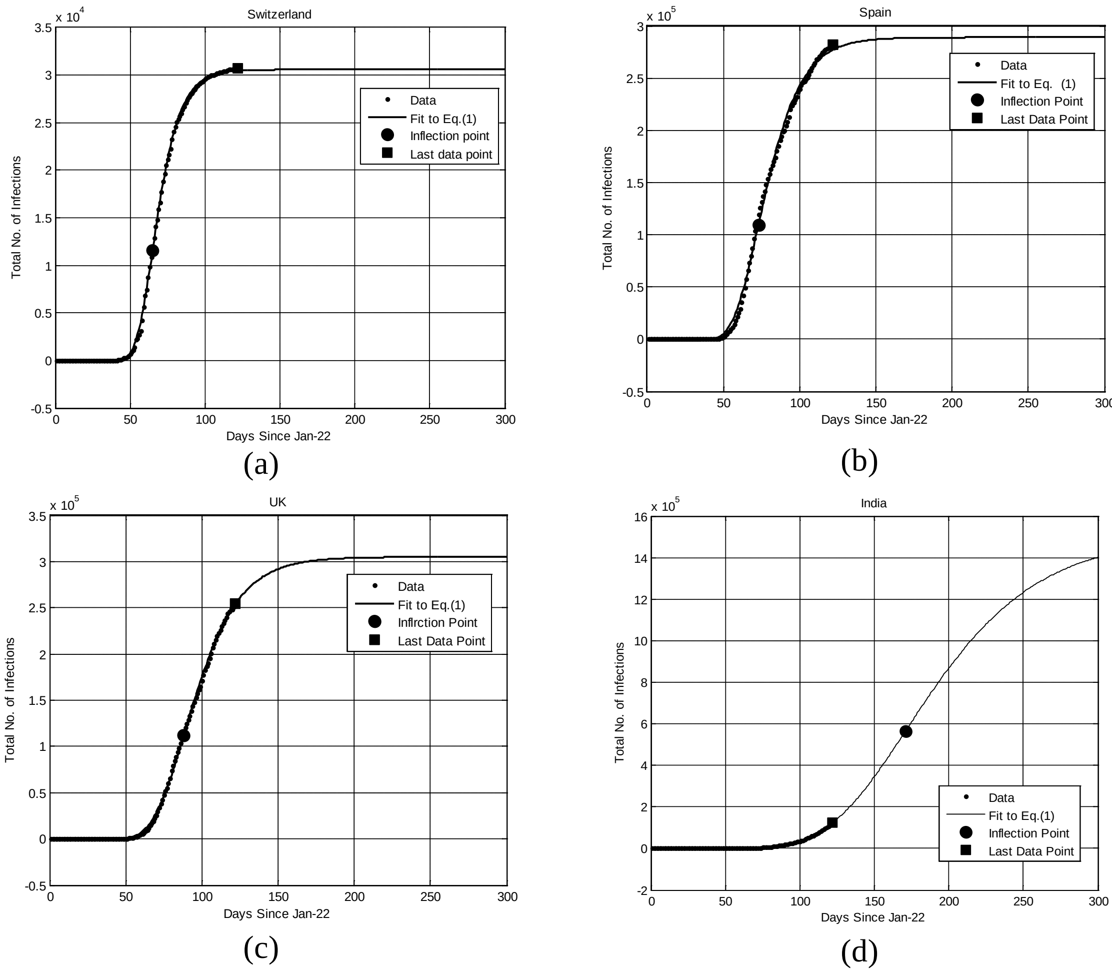

Figure 2. Examples of groups I, II, III, and IV COVID-19 infections data fitted to equation (1). (a) Switzerland. (b) Spain, (c) UK, and (d) India respectively

As it is the case with any empirical fitting procedure, its usefulness is limited to the academic purpose of demonstrating the ability of the suggested empirical equation to describe the data unless the fit is useable in describing situations outside the data domain used in the fit. Equation (1) is shown to provide a reasonable description of all available COVID-19 data. However, the questions on whether fits to this equation can be safely extrapolated to produce estimations on magnitude and date of infections saturation in any particular country still remained unanswered. The following discussion is based on the assumption that there will be no sudden or drastic change in factors affecting the virus spread on the ground. Examples of such factors can be the introduction of a working vaccine or treatment drug, or the sudden abandonment of current social distancing measures. Under such assumption, it can be reasonably argued that the situation with group (I) countries is relatively easy. Once the pandemic in a particular country reaches the saturation part of the curve, flat horizontal extrapolation of the leveling off is trivial. Few fluctuations from the flat leveling off are to be expected of course, but the overall trend will remain the same. For such countries, extracting new information from the fit is limited to the monitoring of any increases in infection above the already achieved leveling off.

The situation with countries where the pandemic is short from reaching leveling off stage is somehow different. As mentioned earlier, the robustness of any fit is highly dependent on the number of data points used. The question is can one safely use the fit extrapolated leveling off horizontal line to predict the ultimate saturation level? The answer is a simple NO. Extrapolations are good enough only in cases of straight lines fittings. Even then, the addition or removal of new points to or from the fitted data can significantly change the slope and intercept of the fitted straight line. The situation with more complicated nonlinear equation like equation (1) fitting is much more difficult. In short, and as far as equation (1) is concerned, the saturation leveling off value is significantly affected by the number of data points used in the fit. To demonstrate this fact, The COVID-19 infections data from Switzerland as an example of a country where leveling off can be considered to have been reached are selected. These data have been showing a good degree of leveling off in numbers of infections for at least a week before May-27-2020. The increase in the number of infections during this week is less than 250, and it represents only 0.8% of the saturation level of 30700 cases. These data can thus be considered a reasonable and perhaps the only available example of being nearest to being leveled off. Multiple fits using equation (1) are performed using Switzerland's data with different number of data points. The smallest set of data points are those which are truncated at the inflection point. One data point is added to the set and the fit is repeated each time until the final available point in the data set is reached. The results of such fits are shown in Figure 2. The main conclusion drawn from such analysis is that the value of the extrapolated curve saturation leveling off is significantly affected by the number of points included in the fit in the region before actual leveling off is achieved. The difference between the extrapolated saturation values for the data truncated at the inflection point and the complete data set is about 20%. Similar analysis for other countries showed similar pattern but with no systematic relation between the curve saturation value and the number of data points used in the fit. Furthermore three important properties regarding the curve inflection point are worth mentioning. The first is that all fits carried out using different truncation levels are identical for the region prior to the inflection point. The second is that for most fits carried out for different countries, the data post inflection point represent about two thirds of the complete data set for that country. The third is that most attempts to carry out fits to equation (1) using data truncated below the inflection point have failed to produce acceptable convergence. This leads to the conclusion that data portion post inflection point have the major important role to play in the fit quality and results.

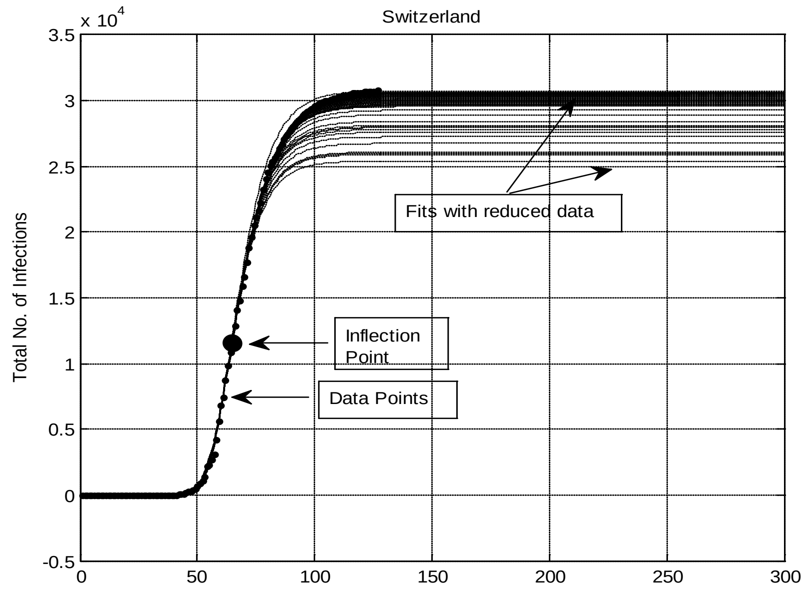

Figure 3. Results of fits with different sizes of truncated data

Figure 3. clearly suggests that the extrapolated behaviors is dependent upon the number of data points used in the fit. It becomes thus necessary to apply some correction to the extrapolated leveling off predictions of equation (1). The correction is based on the assumption that future data daily increases have the same statistical distributions of past data. For such purpose, percentage daily increases in infections for the whole World, Germany, Italy and France are plotted and shown in Figure 3. Results for other countries are much similar. It is clear from this figure that daily percentage increases in the number of infections is always in the range of few percent.

Adopting the above hypothesis that the extrapolated statistical distribution of the percentage daily increases of infections in future data are to have the same statistical distribution as those of the prior data, the mean and the standard deviation for the percentage daily changes for each country is calculated. Ten new projected points belonging to the immediate extrapolated fit are added to the real data set. These projected points are modulated by being lifted up to two different levels. The higher level which represents the worst case scenario. This involves lifting these points up by a percentage equals to the mean plus three standard deviations of the daily increases in infections. The lower level represents the best case scenario where the lifting up is only by a percentage equal to the mean. The reason behind selecting the number ten is to be discussed later. Both sets of modified are fitted to equation (1) and two new extrapolations of leveling are obtained. These represent the upper and lower limit estimation of the projected pandemic development. Sample results of such procedure are shown in Figure (6-c) and (7-c).

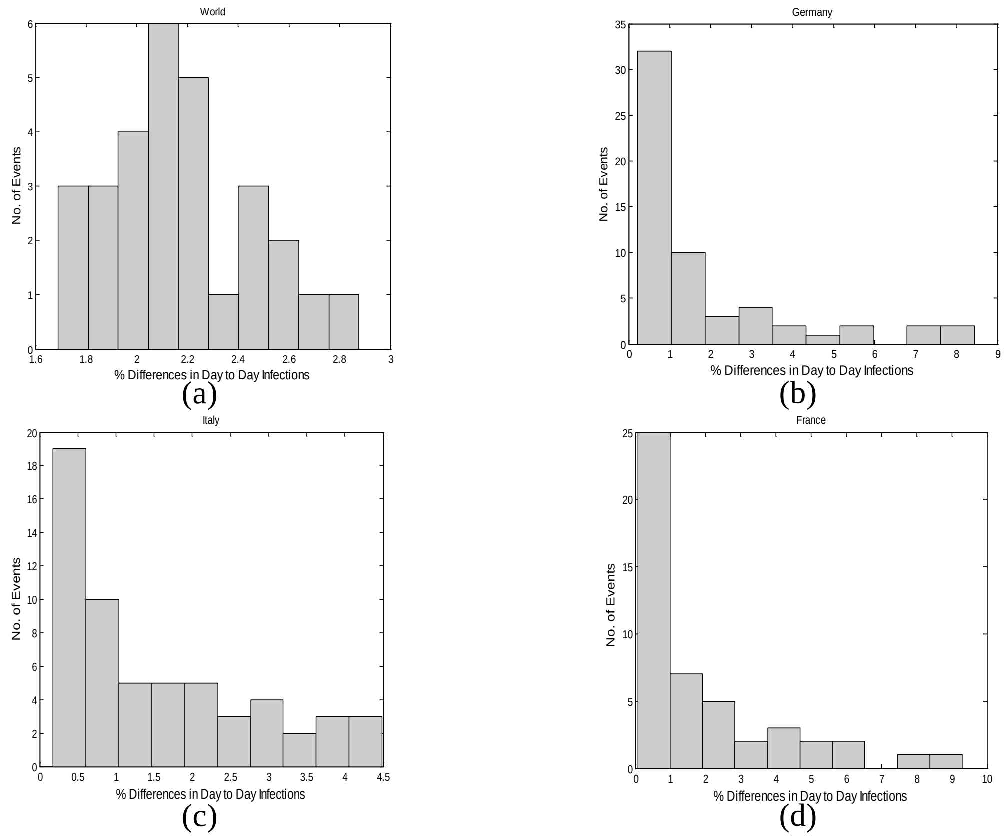

Figure 4. Four examples of the distributions of the percentage daily increases in infections (a) World, (b) Germany, (c) Italy, (d) France.

In order to estimate the approximate date of the leveling off, two points on the upper and lower extrapolated curves are selected such that their values are larger by not more than 0.01% than their immediate predecessor points.

It is important to state that all above analysis is equally applicable for the total number of death cases caused by COVID-19 in any country because death numbers follow almost exactly the same pattern as that of infections.

4 The Software

All above calculations are contained within a free downloadable MATAB code which performs the fitting, calculate the corrections and make the estimations. The software is available on the author's MATLAB file exchange website [23]. The software input data are those for the number of infections or deaths in any particular country. These should be pre-saved as a MATAB data file under a given name. The software is activated by entering the statement

\>> COVID_19(name of data file)

The software package include infections data files for twenty countries and deaths data files for ten countries. These data files are up to date until June-1-2020. The software will output a plot of the actual data, its extrapolated fit to equation (1), and the upper and lower modified ten points, and the two extrapolated fits. Numerical output of the program includes the upper and lower estimated saturation leveling off values together with their estimated dates. The figure title assumes start of data file to be January-22-2020. Other starting dates can be used with changing the plot x-label to the correct date. The software will fail to produce results if the size of the data is too small such that the inflection point obtained from the first fit lays outside the data range. This can happen in countries where the pandemic is still in the early or the fast rise stage and the inflection point has not been reached. Examples of such countries are Chile and India.

5 Model Cross Test

Two types of cross tests are applied to assess the robustness of the modeling and the software. The first involves running the software several times with the addition of different numbers of projected data points above the actual ones. Sets between one and 100 projected data points are added and the analysis is repeated each time. The percentage differences between upper and lower leveling off values are plotted against the number of data points. Typical results for three countries are shown in Figure 5. These and similar plots for other countries indicate the existence of an optimum number of projected points that can be added. Adding this optimum number of points to the data produces maximum separation between best case and worst case leveling off scenarios. In the majority of cases, this optimum number of points fall between 5 and 15. Consequently, the software is set to add ten projected points to the actual data set. This number can be modified easily within the software if necessary.

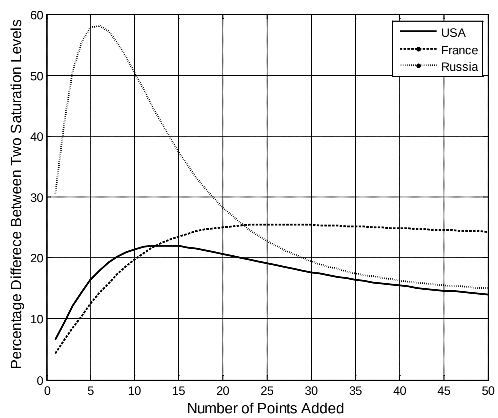

Figure 5: Effect of changing the number of points added to the actual data on the percentage change on the span between upper and lower saturation levels

The second cross check performed is related to the validity of the basic idea of adding projected data points. It is true that projected data points are points inferred from the fitted actual data rather than being real data themselves. To assess the correctness of such procedure, a backward analysis is performed. Analysis related to upper and lower leveling off are carried out using deliberately truncated data. Figures (6 & 7) show two examples of such analysis performed of USA using data truncated on May – 15 and June -1, and for the UK using data which terminate on May-2, and May-17. In both cases, the analysis show that and in spite of the fact that the extrapolated fit leveling off obtained using the truncated data is lower than the corresponding one derived from the full set of available data, the extrapolation is always within the margin between the upper and lower limits projected.

5.1 Model Predictions

After carrying out all above tests and cross checks on the model, it becomes useful to use the model in making some predictions. For this purpose, the software is run on data from nineteen countries which registered the highest infections on June-1-2020 and the world. The software and the data used are available on the MATLAB file exchange website. The data can be updated and used to obtain more accurate predictions. It is worth mentioning that the analysis and the software are equally valid for both infection and mortality data. The summary of result for infections in the countries studied are presented in table (1). Results related to deaths in nine countries and the world are presented in table (2).

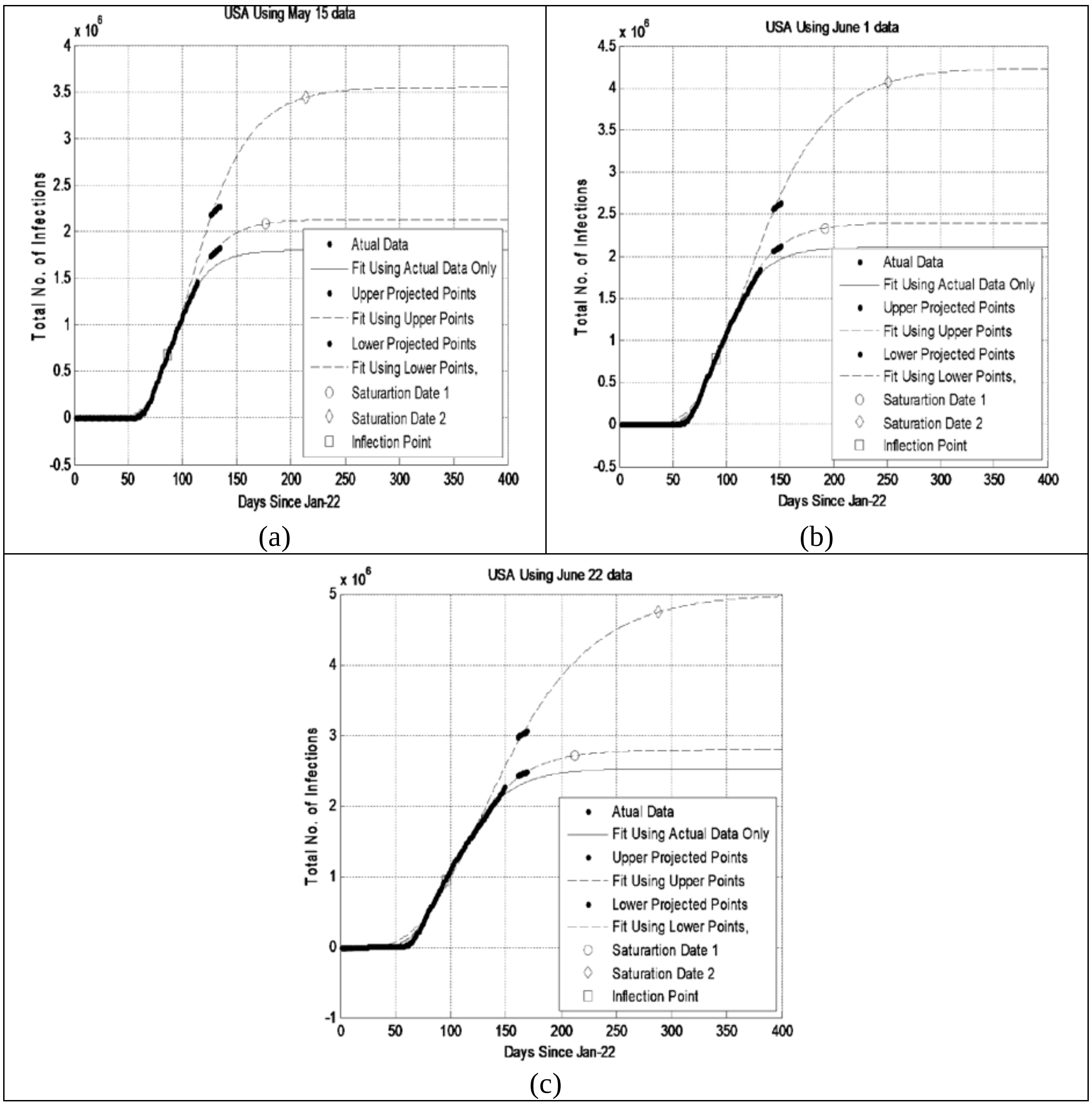

Figure 6: Effect of reduction of number of USA data points on the final model projections

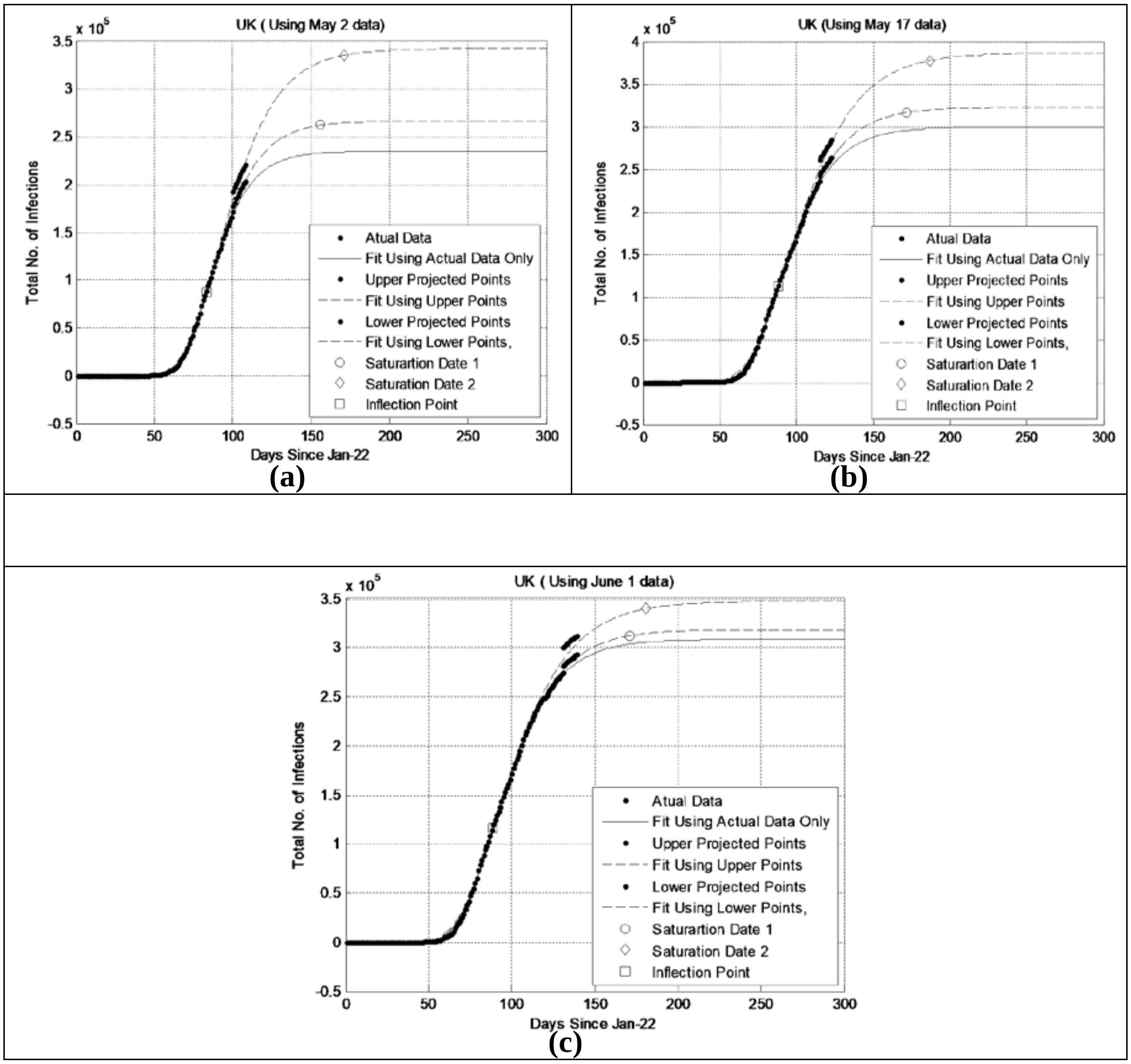

Figure 7. Effect of reduction of number of UK data points on the final model projection

Table 1. Summary of projected total infections leveling off magnitudes and dates in twenty counteries

	Country	Total Infection Cases	Inflection point Days after 22 January	Estimated Upper leveling off	Estimated Lower Leveling off	Estimated Date for Upper Leveling off Days after Jan 22	Estimated Date for Lower Leveling off Days after Jan-22	Comments All data used apart from World and US are up to June 1 2020
	World	**8,908,556**	**128**	**3.6092e+007**	**1.8880e+007**	**307**	**360**	**Data June 22**
1	**USA**	**2,263,651**	**91**	**4.9670e+006**	**2.7916e+006**	**212**	**288**	**Data June 22**
2	**Brazil**	**514,849**	**217**	**1.0388e+008**	**3.1382e+007**	**517**	**517**	**??? Inflection not Reached**
3	**Russia**	**405,843**	**112**	**1.5585e+006**	**7.7941e+005**	**262**	**213**	
4	**Spain**	**286,509**	**73**	**3.9272e+005**	**3.0364e+005**	**180**	**145**	
5	**UK**	**274,762**	**89**	**5.3422e+005**	**3.4004e+005**	**227**	**179**	
6	**Italy**	**232,997**	**68**	**2.9085e+005**	**2.4353e+005**	**166**	**140**	
7	**India**	**190,609**	**197**	**6.228e+008**	**1.1392e+007**	**497**	**497**	**??? Inflection not Reached**
8	**France**	**188,882**	**74**	**2.214e+005**	**1.8963e+005**	**151**	**128**	
9	**Germany**	**183,494**	**70**	**2.1671e+005**	**1.8477e+005**	**152**	**128**	
10	**Peru**	**164,476**	**144**	**1.1735e+007**	**1.1315e+006**	**444**	**313**	**? Close to inflection**
11	**Turkey**	**163,942**	**84**	**2.7261e+005**	**1.7508e+005**	**204**	**152**	
12	**Iran**	**151,466**	**82**	**6.9483e+005**	**1.9311e+005**	**388**	**206**	
13	**Chile**	**99,688**	**???**	**???**	**???**	**???**	**???**	**??? Data not Enough**
14	**Canada**	**90,947**	**93**	**2.163e+005**	**1.2054e+005**	**252**	**191**	
15	**Mexico**	**87,512**	**159 9**	**1.0265e+007**	**1.2164e+006**	**459**	**351**	**??? Inflection not Reached**
16	**Saudi Arabia**	**85,261**	**110**	**1.3912e+006**	**2.6835e+005**	**350**	**238**	
17	**China**	**83,001**	**16**	**82266**	**82266**	**49**	**49**	
18	**Pakistan**	**69,496**	**157**	**1.7755e+008**	**7.594e+005**	**457**	**354**	**??? Inflection not Reached**
19	**Belgium**	**58,381**	**77**	**78025**	**61337**	**175**	**143**	
20	**Qatar**	**56,910**	**146**	**1.5125e+006**	**1.9126e+005**	**435**	**268**	**??? Inflection not Reached**

Table 2. Summary of projected total deaths leveling off magnitudes and dates in twenty countries

	Country	Number of Deaths June 1	Inflection Point	Upper Estimated Deaths Leveling off	Lower Estimated Death Leveling off	Upper Leveling off Data	Lower Leveling off Date
1	**World**	**380,265**	**90**	**6.3256e+005**	**5.2998e+005**	**228**	**203**
2	**USA**	**107,620**	**92**	**2.2587e+006**	**1.2974e+005**	**394**	**183**
3	**Russia**	**5,037**	**135**	**2.6867e+005**	**24,407**	**442**	**292**
4	**Spain**	**27,127**	**74**	**34142**	**29,112**	**161**	**136**
5	**UK**	**39,369**	**87**	**55711**	**43,999**	**198**	**165**
6	**Italy**	**33,530**	**73**	**40014**	**35,137**	**169**	**147**
7	**France**	**28,940**	**79**	**33459**	**29659**	**155**	**136**
8	**Germany**	**8,643**	**84**	**10670**	**9153**	**172**	**149**
9	**Canada**	**7,395**	**101**	**13909**	**9665**	**230**	**188**

6 Discussion and Conclusions

Beside demonstrating the ability of equation (1) in describing the behavior of COVID-19 accumulated infections and deaths data, the devised extrapolation procedure applied provides reasonable future estimations of upper and lower limits of infections and deaths together with approximate dates for the establishment of leveling offs. Furthermore, these estimations are supported by the consistencies of results between infections and deaths. These consistencies can be observed through the comparisons of expected upper and lower saturation dates. These differences are in the range of few days only. One further proved consistency in the predictions is related to group (I) countries which have almost reached saturated leveling off. The model succeeded in predicting the dates when such leveling off have been reached. Examples of such countries are China and Switzerland. These consistencies give added weight to other projected predictions made.

Acknowledgment

The author declares that this work is completely private effort and it has not been supported by any governmental, financial, educational or otherwise establishment.

Conflict of Interest Declaration

The author declares that there is no conflict of interest statement.

Ethics Committee Approval and Informed Consent

The author declares that declare that that there is no ethics committee approval and/or informed consent statement.

References

[1] WHO, Modes of transmission of virus causing COVID-19: implications for IPC precaution recommendations, “https://www.who.int/news-room/commentaries/detail/modes-of-transmission-of-virus-causing-covid-19-implications-for-ipc-precaution-recommendations”

[2] Y. R. Guo, Q. D. Cao , Z. S. Hong , Y. Y. Tan, S. D. Chen , H. J. Jin , K. S. Tan, D. Y. Wang and Yan, The origin, transmission and clinical therapies on coronavirus disease 2019 (COVID-19) outbreak – an update on the status, Military Medical Research (2020) 7:11

[3] S. P. Adhikari , S. Meng , Y. J. Wu , Y. P. Mao , R. X. Ye , Q. Z. Wang , C. Sun , S. Sylvia , S. Rozelle , H. Raat and H. Zhou, Epidemiology, causes, clinical manifestation and diagnosis, prevention and control of coronavirus disease (COVID-19) during the early outbreak period: a scoping review, Infectious Diseases of Poverty (2020) 9:29

[4] S. A. Lauer, K. H. Grantz, Q. Bi, F. K. Jones, Q. Zheng, H. R. Meredith, A. S. Azman, N. G. Reich, J. Lessler, The incubation period of Coronavirus Disease 2019 (COVID-19) from publicly reported confirmed cases: estimation and application, Annals of Internal Medicine 172(9) 2020, 577-582.

[5] WHO, Coronavirus disease 2019 (COVID-19) Situation Report – 73 “https://www.who.int/docs/default-source/coronaviruse/situation-reports/20200402-sitrep-73-covid-19.pdf?sfvrsn=5ae25bc7_4”

[6] CDC, Interim Clinical Guidance for Management of Patients with Confirmed Coronavirus Disease (COVID-19), “https://www.cdc.gov/coronavirus/2019-ncov/hcp/clinical-guidance-management-patients.html”

[7] K. Ozkan “How close are we to a Covid-19 vaccine?” J. Pure Appl. Microbiology, 14(Special Edition), 2020, 6201

[8] N. Lurie, M. Saville, R. Hatchett, and J. Halton “Developing Covid-19 Vaccines at Pandemic Speed” The New England Journal Of Medicine 382(21) 2020, 1969-1973.

[9] M. Singh, P. Sarkhel, G. J. Kang, A. Marathe, K. Boyle, P. Murray-Tuite, K. M. Abbas and S. Swarup, Impact of demographic disparities in social distancing and vaccination on influenza epidemics in urban and rural regions of the United States, BMC Infectious Diseases 19 (2019), 221

[10] P. Suppawittaya , P. Yiemphat , P. Yasri, Effects of social distancing, self-quarantine and self-isolation during the COVID-19 pandemic on people’s well-being, and how to cope with it, International Journal of Science and Healthcare Research, 5(2) 2020, 12-20

[11] J. A. Lewnard and N. C. Lo, Scientific and ethical basis for social-distancing interventions against COVID-19, Lancet Infect Dis. 2020

[12] B. Ivorra , M. R. Ferrández, M. Vela-Pérez, A.M. Ramos, Mathematical modeling of the spread of the coronavirus disease 2019 (COVID-19) taking into account the undetected infections. The case of China, Commun Nonlinear Sci Numer Simulat 88 (2020) 105303

[13] Y. Li, B. Wang, R. Peng, C. Zhou, Y. Zhan, Z. Liu, X. Jiang and B. Zhao “Mathematical modeling and epidemic prediction of COVID-19 and its significance to epidemic prevention and control measures” Annals of Infectious Disease and Epidemiology, 5 (1) 2020, Article 1052

[14] J. Panovska-Griffiths “Can mathematical modelling solve the current Covid-19 crisis?, BMC Public Health (2020) 20:551

[15] K. Liang, Mathematical model of infection kinetics and its analysis for COVID-19, SARS and MERS” Infection, Genetics and Evolution, 82, 104306

[16] Zafer Cakir, Hasan Basri Savas “A Mathematical Modelling Approach in the Spread of the Novel 2019 Coronavirus SARS-CoV-2 (COVID-19) Pandemic” Electronic Journal of General Medicine 17(4) 2020,

[17] S.Kim, Y. Seo, E. Jung, Prediction of COVID-19 transmission dynamics using a mathematical model considering behavior changes in Korea, Epidemiology and Health Volume: 42, Article ID: e2020026.

[18] A. J. Kucharski, T. W. Russell, C. Diamond, Y. Liu, J. Edmunds, S. Funk, R. M. Eggo, Early dynamics of transmission and control of COVID-19: a mathematical modelling study, The Lancet Infectious Diseases, 2020, 553-558

[19] N. P. Jewel, Predictive mathematical models of the COVID-19 pandemic underlying principles and value of projections, Journal of the American Medical Association, 323(19) 2020, 1893-1894.

[20] A.R. Tuite, D. N. Fisman, A. L. Greer, Mathematical modelling of COVID-19 transmission and mitigation strategies in the population of Ontario, Canada, 11 (192) 2020, 497-505

[21] Word meter website https://www.worldometers.info/coronavirus/

[22] https://www.mathworks.com/campaigns/products/trials.html

[23] https://www.mathworks.com/matlabcentral/profile/authors/277505-aasim-azooz

Asim A. Azooz, ORCID: https://orcid.org/0000-0001-7084-9518

Journal of Multidisciplinary Modeling and Optimization 3(1) (2020), 27-34.

Some Applications of Free Group

Karim S. KALAF[1], Hekmat Sh. MUSTAFA[2]
and Majid Mohammed ABED[3]

[1] Department of Mathematics,
University of Anbar, Anbar, Iraq
Karem.saber@uoanbar.edu.iq

[2]Department of Mathematics,
University of Al-Hamdaniya, Mosul, Iraq
hekmat78@uohamdaniya.edu.iq

[3]Department of Mathematics,
University of Anbar, Anbar, Iraq
majid_math@uoanbar.edu.iq

Received: 31.07.2020, Accepted: 16.09.2020, Published: 17.09.2020

Abstract — *In this paper, we study many concepts as applications of free group, for example, presentation, rank of free group, and inverse of free group. We discussed some results about presentation concept and related it with free group. Our main result about free rank, is if G is a group, then G is free rank n if and only if $G \cong Z^n$. Also, we obtained a new fact about inverse semigroup which say there is no free inverse semigroup is finitely generated as a semigroup. Moreover, we studied some results of inverse of free semigroup.*

Keywords: Free group, Finite group, Semigroup, Rank freegroup, Inverse free semigroup.
Mathematics Subject Classification: 20M25, 20E05.

1 Introduction

Several authors have investigated the free group. Sury in [1], defined a free group F on a set X by the universal property that abstract map from X to any group G can be extended uniquely as a homomorphism from F to G. Note that a group G is free abelian of rank n if f $G \cong Z^n$.

Derek Holt introduced the definition generate of subgroup by the following, for all $X \subseteq G$ with G is a group we say a subgroup $\langle X \rangle$ of G generated by X in two ways, $\langle X \rangle$ is intersection of all subgroup H of G that contains X, *i.e.*, $\langle X \rangle = \cap_{H \leq G, X \subseteq H} H$ and if $X^{-1} = \{x^{-1} \mid x \in X\}$, then $A = X \cup X^{-1}$. We say A^* to be the set of all words over A. Elements of A^* represent elements of G, it is closed under concatenation and inversion. So, it is a subgroup of G. So $\langle X \rangle = A^*$. In [1], the empty word represents 1_G introduced in details. Also, in [2], we found proof of the following, a finite group G is not free if $G \neq \{1\}$.

In [3], Jairo Gon, calves studied the existence of free subgroups in unit groups of matrix rings and group rings.

Cite as: *K. S. Kalaf, H. Sh. Mustafa, M. M. Abed, Some Applications of Free Group, Journal of Multidisciplinary Modeling and Optimization 3(1) (2020), 27-34.*

Charles F. Miller In [4], proved that every group is a quotient group of a free group and then if G is a group there is a free group F and a normal subgroup N such that $G\cong F/N$. Let G be an abelian group and $S=\{x_1,\dots, x_t\}$ be a subset of G. We said S linearly independent if for each $n_1,\dots,n_t$ belong Z and $n_1x_1,\dots,n_ix_i=0$, then for all $1\leq i\leq t$ [2]. Let G be an abelian group, then G is called a finitely generated free group if G has a finite basis (see [1]). Let S and S^{-1} be two sets such that $sns^{-1}=\phi$, $|s|=|s^{-1}|$. If $s^{-1}\in S$ is a unique elements of s in S for all $s\in S^{-1}$ and $t^{-1}\in S$ is a unique element of $t\in s^{-1}$, then $((s^{-1})+1=s)$, for all $s \in S$ [3]. Let $H\leq G$, then H is a free subgroup and $F(S) = Z$ is a free group.

In [5], Maltsev, studied the equation $zxyx^{-1}y^{-1}z^{-1} = aba^{-1}b^{-1}$ in a free group. Also, in [6] the authors studied the periodic automorphisms of free groups in details. Periodic automorphisms of the two-generator free group was investigated by Meskin in [7].

In this article, we introduced some applications of free group and some new results which explain the relationships between several concepts and free group.

2 Presentation of Free Group

Here we discuss some results about presentation concept and related it with free group. Let $G=\langle S\rangle$ and $F(S)=\langle S\rangle$ is a *F-group*. Let $R\subseteq F(S)$ and $N=\langle R\rangle$ be normal subgroups of free group F(S) which generated by set R in other words, $N=\langle\{a^{-1}ra:a\in F(S), r\in R\}\rangle$.
Let $\varphi:F(S)\to G$ be onto homomorphism. So $\langle S,R\rangle$ is presentation of G if Ker $\varphi=N$, i.e. $F(S)/N\cong G$. If S,R are finite sets, then $\langle S,R\rangle$ is a finite presentation of G.

Remark 2.1. Every element in F(S) is called realtor.

Note that the presentation of a group is a different from representation of free group. Therefore, a presentation of a group G is an expression of Gas a quotient of a free group.

Example 2.2. $G\neq\langle a, b|a^2=1, b^3=1\rangle$, then we say G is the quotient $F/N \ni F$ is the free group of rank 2 generated by $\{a, b\}$ and N is the smallest normal subgroup of F containing the element $a^2$and b^2.Also, we can describe the group Gabove as the free product $Z_2\times Z_3$. Then $a\neq\langle a,b|a^2=1, aba^{-1}b^{-1}=1\rangle\cong Z_2\times Z$. If we add a new relation, then we cannot change the group. See the following $G\neq\langle a,b|a^2=1, ab^2a^{-1}b^{-1}, ab^2a^{-2}b^{-2}=1\rangle$ and $G=\langle a_1, a_2,\dots,a_n\rangle|r_1=r_2=\dots r_m=e\rangle$ and if r is a word $r^1(r_2)^{-1}$, then we are *write* $r_1=r_2$ as a replacement to $r=e$.
Remark 2.3. There is no unique presentation of group (there is many presentations of group G. See the following example:

Example 2.4. It is clear $Z_5=\langle a|a^5=e\rangle$ because:

$$\begin{aligned}
&\langle a, b, c|ab=c, cb=a, bca=b\rangle\\
&=\langle a, b. c|ab=c, cbc=a, ca=e\rangle\\
&=\langle a, b, c|ab=c, cbc=a, c=a^{-1}\rangle\\
&=\langle a, b|ab=a^{-1}, a^{-1}ba^{-1}=a\rangle\\
&=\langle a, b|b=a^{-2}, a^{-1}ba^{-1}=a\\
&=\langle a|a^{-1}a^{-2}a^{-1}=a\rangle
\end{aligned}$$

$$=\langle a|a^5=e\rangle.$$

Theorem 2.5. Let $G=\langle S|R\rangle$ and $H=\langle S|R_1\rangle$ such that $R\subseteq R_1$ then H is isomorphic of quotient group.

Proof. Suppose that F=F(S) and N, $N_1$are two normal subgroups of F which are generated by two sets R and $R_1$and, respectively. Since $R\subseteq R_1$, then $N\leq N_1$.Since $N\lhd F$ *then* $N\lhd N_1$. Since $G\cong F/N$ and $H\cong (F/N)$ then by (The Third Theorem of Isomorphism), we get $H\cong F/N\cong (F/N)/(N_1/N)\cong G/N_1$. We can get presentation of group G by other presentation of other group G_1 especially G finite group.

Lemma 2.6. If $G=<S|R>$and $H=<S|R_1>$such that R subset of R_1, then H isomorphic quotient of free group G.

Proof. Suppose that F=$F(S)$ and let N, N_1 be two normal subgroups of F and generated by R and R_1. Since R subset of R_1, then N subgroup of N_1. Also, since $N\trianglelefteq F$, then $N\trianglelefteq N_1$. We have $G\cong(F/N)$ and $H\cong(F/N)$, therefore from The Third Theorem of Isomorphism we get

$$H=F/N_1\cong(F/N)/(N_1/N)\cong G/N_1$$

Corollary 2.7. Let $\langle S,R\rangle$ be finite group and let H be a group satisfying $|Q|\leq|H|$. Let $T\subseteq H$ be a set of generators such that $Q:S\rightarrow T$ and $(S_2)^{a2},\ldots,(S_n)^{an}$, implies to $Q(S_2)^{a1},Q(S_2)^{a2},\ldots, Q(S_n)^{an}=e$, *then* $G\cong H$.

Proof. Note that $G\cong\langle T|Q(R)\rangle$*and* $H=\langle T|Q(R)\rangle\cup R_1\rangle$. From Lemma 2.6, we obtain $H\cong G/N$ such that $N\trianglelefteq G$. Thus $|G|=|H||N|$. Since $|G|\leq|H|$, then $|N|=1$ and hence $|N|=\{e\}$. Thus $H\cong G$.

Corollary 2.8. Let $G\langle a,b|a^2=e, b^3=e, (ab)^2=e\rangle$. Then $G\cong S_3$.

Proof. Suppose that $N=\langle b\rangle$. Since $(ab)^2=e$, then $a^{-1}b^{-1}a=b\in N$, *also* $b^{-1}bb=b\in N$. Thus $N\trianglelefteq G$. Now $G/N=G/\langle b\rangle\cong\langle a, b|a^2=e, b^3=e, (ab)^2=e, b=-e\rangle=\langle a|a^2=e\rangle\cong Z_2$. *Since* $|N|=3$, *then* $|G|\leq 6$. *But* $S_3=\langle(1\ 2), (1\ 2\ 3)\ni(1\ 2)\circ(1\ 2\ 3)^2=(1)$ *and* $|S_3|=6$. *Thus* $G\cong S_3$.

Corollary 2.9. Let $\langle a, b|a^n=e, b^m=e, ab=ba\rangle$ then $G\cong Z_n\times Z_m$.

Proof. Since ab=ba then G is commutative group. Suppose that $N=\langle a\rangle$. Hence $N\trianglelefteq G$ and $G/N=\langle a,b|a^n=e,\ b^m=e,ab,ba,a=e\rangle=\langle b|b^m=e\rangle\cong Z_m$. Since $|N|\leq n$, then $|G|\leq nm$. Now $Z_n\times Z_m=\langle[1], [0], [1]\rangle$ such that $m([0], [1])=([0],[0])n$, $([1], [0])=([0], [0])$ and $([1], [0])+([0], [0])=([0], [1])+([1],[0])$. Thus $G\cong Z_n\times Z_m$.

Corollary 2.10. Let $G=\langle A, B\rangle\leq GL(2, R)\ni A=\begin{bmatrix}1 & 0\\ -1 & 0\end{bmatrix}$, $B=\begin{bmatrix}0 & 1\\ 1 & 0\end{bmatrix}$. Then $G\cong D_4$.

Proof. Note that $A^4=\begin{bmatrix}0 & 1\\ 1 & 0\end{bmatrix}$, $B^2=\begin{bmatrix}-1 & 0\\ 0 & 0\end{bmatrix}$ and $BA=A^3B=\begin{bmatrix}-1 & 0\\ 0 & 0\end{bmatrix}$. Thus $G=\langle A,B,A^4=I, B^2=I,BA=A^3B\rangle$. Suppose that $N=\langle A\rangle$. Since $A^3=A^{-1}$and $BA=A^3B=A^{-1}B$, then $BAB^{-1}=A^{-1}\in N$. Also, $AAA^{-1}=A\in N$ and so $N\trianglelefteq G$ and hence $G/N=\langle A,B|A^4=I,B^2=I,\ BA=A^3B,$

$A=I\rangle=\langle B|B^2=I\rangle=Z_2$. Since $|N|\leq 4$, then $|G|\leq 8$. But $D_4=\langle a, b|a^4=e, b^2=e, ba=a^3b\rangle$ and $|D_4|=8$. Thus $G\cong D_4$.

Corollary 2.11. Let $G=\langle a, b|a^2=b^3=e, (ab)^n=(ab^{-1}ab)^k\rangle$. Then

1. $G=\langle ab, ab^{-1}ab\rangle$
2. $\langle (ab)^n\rangle\leq G$.

Proof.

1. Suppose that $H=\langle ab, ab^{-1}ab\rangle\leq G$, then $ab^{-1}=ab^{-1}ab(ab)\in H$, and $a=abb\text{-}1\in H$, then $H=G$.
2. Suppose that $M=\langle(ab)^n\rangle\leq G$. To prove $M\leq G$ we need by (1) prove that $[(ab)^n, ab]=e$ and, $[ab]=(ab)^{-n}(ab)^n(ab)=(ab)^{-(n+1)}(ab)^{n+1}=e$. Hence $(ab)^n=(ab^{-1}ab)^k=(a^{-1}b^{-1}ab)^k\in G$. Thus, $M\leq G$.

Theorem 2.12. Let $G=\langle a,b\rangle$ such that $x^3=e$, for all x in G. Then

1. $[a,b]\in Z(G)$.
2. G is a finite group.

Proof.

1. To prove $[a, b]\in Z(G)$, we should prove that $[a,b]$ *commutator* with a,b. Now

$$\begin{aligned} a^{-1}[a, b] &= a\text{-}1(a^{-1}b^{-1}ab) \\ &= a(b^{-1}a)ba \\ &= a(a^{-1}ba^{-1}b)ba \\ &= ba^{-1}b^{-1}a \\ &= b(baba)a \\ &= b^{-1}aba^{-1} \\ &= a^{-1}ba^{-1}bba^{-1} \\ &= a^{-1}ba^{-1}b^{-1}a^{-1} \\ &= a^{-1}ba^{-1}b^{-1}a^{-1} \\ &= a^{-1}ba^{-1}b^{-1}a^{-1} \\ &= a^{-1}ba^{-1}bba^{-1} \\ &= a^{-1}ba^{-1}b^{-1}a^{-1} \\ &= a^{-1}ba^{-1}b\text{-}1a^{-1} \\ &= a^{-1}bbabaa^{-1} \\ &= a^{-1}b^{-1}ab \\ &= [a, b] \end{aligned}$$

Thus $[a,b]a=a[a,b]$ and by similarly $[a,b]b=b[a,b]$ and *so* $[a, b]\in Z(G)$.

2. Since $[a,b] \in Z(G)$, then $G/Z(G)$ commutative group. Therefore, any commutative group generated by a finite set and satisfying $x^n=e$ such that $n \in Z^+$. Then $G/Z(G)$ is a finite. So, $G/Z(G)$, $Z(G)$ are finite groups. Thus $G$is a finite group.

3 Rank of Free Group

In this subsection, we study another application of free group, namely, the rank of $abelian$ group. We can use a generalized linear algebra, therefore we will discuss the factors of integers Z. Let G be an $abelian$ group. Then the set of $n distint elements$ $\{g_1,\ldots,g_n\}$ subset of G is called Z $lineraly$ independent and we have $\sum r_i g_i=0$, $i=1,\ldots,n$. If and only if $r_1=r_2=\ldots=r_n=0$.

Definition 3.1 Let G be an $abelian$ group. Then the rank of G is the size of the largest set of Z-$lineraly$ independent elements in G.

Remark 3.2 Let G be an abelian group. Then G is called free of rank n if G has a set of n linearly independent generators. Moreover, the set of generators is called basis for G.

Theorem 3.3 Let G be a group. Then G is free rank n if and only if $G \cong Z^n$.

Proof. Let $g_1,\ldots,g_n$ be a basis for G , and let α:$Z^n \rightarrow G$ such that $\alpha(r_1,\ldots r_n)=\sum r_i g_i$, $i=1,\ldots,n$. Since x is surjective homomorphism, therefore we need to prove that $\alpha$is injective. Let $(r_1,\ldots,r_n)$ belong to Ker(α), then by definition $\sum r_i g_i=0$, $i=1,\ldots,n$. Now since g_i are linearly independent, then $r_i=0$ for all i and so $(r_1,\ldots,r_n)=(0,\ldots,0)$. Thus Ker(x)=$\{0\}$ and this means α is injective and then is isomorphism.

Corollary 3.4 Let G be an abelian group. If G is n-generated, then rank (G)$\leq$n.

Proof. Suppose that $x:Z^n \rightarrow G$ be an onto all g_i are linearly independent. Since α is onto, then there exists $h_1,\ldots,h_k$ belong to Z^n andα $(h_i)=g_i$. Suppose that$\sum r_i h_i=0$. Therefore by α we get: $0=\alpha(\sum r_i h_i)=\sum r_i \alpha(h_i)=\sum r_i g_i$, $i=1,\ldots k$. Since g_i is a linearly independent, then, $r_1=r_2=r_3=0$ and this implies that $h_i=0$. Also, linearly independent, but $k \leq n$ and so rank (G)$\leq$n.

Example 3.5 If $F_n$is F-group has rank n, then F_n contain sub-F-group F_k, for all $1 \leq k \leq n$. If $S_n=\{S_1,\ldots,S_n\}$ and if $S_k=\{S_1,\ldots,S_k\}$, we get $F_k=F(S_k) \leq F(S_n)=F_n$.

Remark 3.6 We call S is a free basis of F of and the order of S is a rank of free group F_n . If $|S|=n$, then F is a free group has rank n and denoted by F_n.

Corollary 3.7. Let G_1 and G_2 be an abelian group with finite rank. Then $\text{rank}(G_1 \times G_2) \geq$ rank (G_1)+rank(G_2)

Proof. Let $rank(G_1)$ $=k$ and $rank(G_2)=h$. Suppose $g_1,\ldots,g_n$ belong to G_1 such that are linearly independent. Also suppose $g_1,\ldots,g_n$ be a linearly independent. Therefore we can claim linearly $(g_1,0),\ldots,(g_k,0)$, $(0, s_1),\ldots,(0, s_n)$ are linearly independent in $G_1 \times G_2$. Now suppose that

$$\sum r_i(g_i+0)\sum b_j(0, h_i)=(0, 0), j=1,\ldots h.$$

Therefore, by linear independence we have $r_1=r_2=\ldots=r_k=0$ *and* $b_1=b_2=\ldots b_n=0$, as desired.

Theorem 3.8 Let n be a positive integer number and let F_{n+1} be *F-group* has rank *(n+1).* Then there exists image homomorphism G of group F_{n+1} $G\cong F_n$.

Proof. Suppose that $F_{n+1}=F(S)$ such that |S|=n+1. Let $S=S_1\cup\{\alpha\}$ such that $|S_1|=n$. It is clear $G=G(S_1)\leq F(S_1)$ and $\varphi:S\rightarrow G$ which define by $\varphi(x)=\begin{cases}x, x\neq a\\ e, x=a\end{cases}$

Can be extended into onto homomorphism φ:F(S) → G, thus F_{n+1} $G\cong F_n$.

Theorem 3.9 Let be a free group with rank *n*. Then F_n contains subgroup with index m for each m $\in Z^+$.

Proof. Suppose that G⟨a⟩ is a finite cyclic group with order m and let F_n = F(S) such that S={$s_1,\ldots s_n$} then there exists onto homo$\varphi:F_n\rightarrow G$ and satisfying φ(Si)=a, for all $1\leq i\leq n$. Then by (First Theorem of Isomorphic) we get $F_n/\ker\varphi\cong G$. Thus $Ker\varphi\leq F_n$ with index *n*.

Let G be a free abelian group with *Z-basis X* In this case we can say the rank of G is the cardinality of the basis X. The next example shows some properties of Z-basis:

Example 3.10 We know that Z is free abelian group of Z has cardinality one.

Remark 3.11

1. Only cyclic generators of Z are *{1, -1}* and this mean *Z* has only two basis {1} and *{-1}*.
2. Note that {2, 3} is a generating set of *Z* and not contain a *Z-basis* of *Z* as a subset.
3. Note that {2} is a *Z-independent* subset of *Z* and cannot be extended to *Z-basis* of *Z*.

4. Inverse of Free Semigroup

In this subsection, we will study some results of inverse of free semigroup, but before that we should discuss a concept of inverse of semigroup. A study of inverse elements in semi-group very important in this section.

Definition 4.1 An element y belong to *S* is called inverse element of x in *S*, if *x=xy* and *y=yxy*.

Remark 4.2 The inverse element of x in *S* need not be unique.

Lemma 4.3 Any regular element of x in a set *S* has an inverse element.

Proof. Let s be an element in *S* such that s is regular, therefore:

For some *s* in *S*, $t=tst$. Now $sts=sts.t.sts$ and so *sts* is also regular element. Now $t=t.sts.t=t.sts.t$ and sts is an inverse element of *t*.

Now we transition from inverse element to inverse semigroup *S*.

Definition 4.4 Let S be a semigroup. Then S is called an inverse semigroup, if for all s belong to S has a unique inverse element s^{-1} such that $s=sss^{-1}$ *and* $s^{-1}=s^{-1}ss^{-1}$.

Example 4.5 Let S be a group. Then it is an inverse semigroup and the inverse of an element s is s^{-1}.

Theorem 4.6 *Let $S=[X]$.* If generator s in X has unique inverse element. Then S is an inverse semigroup $(s_1s_2\ldots s_n)^{-1} = (sn)^{-1},\ldots,s^{n-1})^{-1}$, s_i *in* X.

Proof. Suppose that x, y $\in$ S and have unique inverse elements s-1 and t^{-1}, respectively. Therefore $st.t^{-1}s^{-1}.st=s1tt^{-1}.s\text{-}1s.t=ss^{-1}s.tt^{-1}.t=st$.

Corollary 4.7 For all x in S such that S is inverse semigroup, then $s=(s^{-1})^{-1}$.

Remark 4.8 For a semigroup S, we have the following statements are true:

1. Let S be a semigroup. An element $a\in S$ is said to be regular if there exists $s\in S$ such that $a=asa$. The elements is an inverse of a if $a=asa$ and $s=sas$.

2. If s is an inverse of a, then the elements ax and xa are idempotents in S. i.e. as=sas and sa=sasa.

3. We say that the semigroup S is inverse if a unary operation $s_1 \rightarrow s^{-1}$ is definitions with the properties; $\forall s, t \in S(s^{-1})=s, ss^{-1}s=ss^{-1}tt^{-1}=tt^{-1}ss^{-1}$.

4. Let s be nonempty set and $X^{-1}=\{s^{-1}:s\in X\}$ be a set in one-one correspondence with X and disjoint from it.

5. Let $Y=X\cup X^{-1}$and consider Y^+ the free semigroup on Y. We define the inverse for the elements of Y^+ by the result $(s^{-1})^{-1}$, $s\in X$. Also $(t_1,\ldots,t_n)^{-1}=(t_n)^{-1},\ldots,(t_n)^{-1}$, $t_1,\ldots,t_n\in Y$, and for any $w\in Y^+$ $(w^{-1})^{-1}=w$.

6. Let T be the congruence generated by the set $T=\{(w^{-1}w, w):w \text{ in } Y^+\}\cup\{ww^{-1}zz^{-1}, zz^{-1}ww\text{-}1):w, z \text{ in } Y^+\}$, Y^+/T is a semigroup under the multiplication $(Wt)(Zt)=(wz)T$, w, z *in* Y^+. The map$:X\rightarrow(Y^+/T)$, $s\rightarrow sT$, is obviously well-defined and is the mapping that we associate to Y^+/T to prove that this inverse semigroup is in fact the free inverse semigroup.

7. Let Sbe any inverse semigroup and φany map from X into S. We can extend φ to Y by defining $s^{-1}\varphi=(s\varphi)^{-1}s\in X$, where $(s\ \varphi)^{-1}$is the inverse of $s\varphi \in S$. Since Y^T is the free semigroup on Y, we can define a semigroup $\varphi_1:Y^T\rightarrow S$ by the rule $(t_1t_2\ldots t_n)\ \varphi_1 = t_1\varphi t_2\varphi$, t_1, t_2, $\ldots,tn \in Y$.

Corollary 4.9 There is no free inverse semigroup is $f.g$ as a semigroup.

Proof. Let $X\neq\emptyset$ be a set and FI_X is defined by the S-group presentation $\langle Y/R\rangle$, where Y and R are finite. If X is infinite. Let $s\in X$ not occurring in the relations of R, then the relation $s=s^{-1}$does not hold in FI_X, this is a contradiction, so X must be finite. We may express each element in Y as a product of elements in X, so $Y=X$. Let use the finite set of relations $\{s_i=s_j: s_i, s_j \in X, i \neq j\}$, we are identifying all the elements of X as a unique element, so we obviously obtain the free inverse semigroup, but this semigroup is not finitely generated and so FI_X is not finitely generated.

Remark 4.11 Let S be an inverse semigroup. Then we have the following is true in general:

$s \le t \Leftrightarrow \exists\ e: t=te \Leftrightarrow ss^{-1}=ts^{-1} \Leftrightarrow s=st^{-1}s= \Leftrightarrow ss^{-1}=st^{-1} \Leftrightarrow ss^{-1}=t^{-1}s \Leftrightarrow t^{-1}s \Leftrightarrow s^{-1}t \Leftrightarrow s=ss^{-1}t.$

Acknowledgment

The authors declare that this work is completely private effort and it has not been supported by any governmental, financial, educational or otherwise establishment. The authors would like to thank the referee, whose careful reading and thoughtful comments have helped improve the paper.

Conflict of Interest Declaration

The authors declare that there is no conflict of interest statement.

Ethics Committee Approval and Informed Consent

The authors declare that declare that that there is no ethics committee approval and/or informed consent statement.

References

[1] B.Sury, Free groups – basics, Stat-Math Unit Indian Statistical Institute Bangalore, India, IIT Bombay, (2010).

[2] B. Baumslag and B. Chandler, Outline of Theory and Problems of Group Theory, New York University, Schaum's Outline Series, Mcgraw-Hill Book Company, New York, San Francisco, Toronto, Sydney, (1986).

[3] J. Z. Gon¸calves and D. S. Passman, Linear groups and group rings, J. Algebra 295 2006, 94–118,

[4] C. F. Miller,Combinatorial Group Theory III, Australian National University, (2004).

[5] A. I. Maltsev, On the equation $zxyx-1\ y-1\ z-1 = aba-1\ b-1$ in a free group, Algebra and Logic, 1(5) 1962, 45-50.

[6] J. L. Dyer and G. P. Scott, Periodic automorphisms of free groups, Comm. Alg., 3 (1975), 195-201.

[7] S. Meskin, Periodic automorphisms of the two-generator free group, in: Proc. Conf. Canberra, 1973 (Lecture Notes in Math., 372 (1974), 494-498). Berlin: Springer.

Karim S. Kalaf, ORCID: https://orcid.org/0000-0002-2632-9141
Hekmat Sh. Mustafa, ORCID: https://orcid.org/0000-0002-4774-2971
Majid M. Abed, ORCID: https://orcid.org/0000-0003-0483-2093

Journal of Multidisciplinary Modeling and Optimization 3(1) (2020), 35-46.

A New Three-Term Conjugate Gradient Algorithm Based on the Dai-Liao and the Liu-Xu Conjugate Gradient Methods

Khalil K. ABBO[1] and Aynur J. NAMIK[2]

[1]Department of Mathematics,
Telafer University, Mosul, Iraq
kh_196538@yahoo.com

[2]Department of Mathematics
Mosul University, Mosul, Iraq
aynoor.Javdet@gmail.com

Received: 01.07.2020, Accepted: 31.08.2020, Published: 17.09.2020

Abstract — *Based on the Dai-Laio and Liu-Xu methods, we develop a new three-term conjugate gradient method for solving large-scale unconstrained optimization problem,. The suggested method satisfies both the descent condition and the conjugacy condition. For uniformly convex function, under standard assumption the global convergence of the algorithm is proved. Finally, some numerical results of the proposed method are given.*

Keywords: Unconstrained optimization, Descent methods, Conjugate Gradient methods.
Mathematics Subject Classification: 65K10, 90C26.

1 Introduction

We deal with the following unconstrained optimization problem:

$$\min f(x), \quad x \in R^n \tag{1}$$

where $f : R^n \to R$ is continuously differentiable and it‘s gradient $g = \nabla f$ is available. there are many different theories and algorithms that have been presented to solve problem (1), (see [1-4]). For solving problem (1), the iterative method is widely used and it‘s form is given by

$$x_{k+1} = x_k + s_k, \quad s_k = \alpha_k d_k, \qquad k = 1,2,..., \tag{2}$$

where $x_k \in R^n$ is the $k-$th approximation to a solution of (1). $\alpha_k \in R$ is a step-length usually chosen to satisfy certain line search conditions [18]. and $d_k \in R^n$ is the search direction and defined by

Cite as: *K. K. Abbo and A. J. Namik, A new three-term conjugate gradient algorithm based on the Dai-Liao and the Liu-Xu conjugate gradient methods, Journal of Multidisciplinary Modeling and Optimization 3(1) (2020), 35-46.*

$$d_{k+1} = -g_{k+1} + \beta_k d_k \quad , \quad d_1 = -g_1$$

where $\beta_k \in R$ is a parameter which characterizes the conjugate gradient method. For general nonlinear functions, different choices of β_k lead to different conjugate gradient methods. Well-known formulas for β_k are called the Fletcher-Reeves (FR) [10], Hestenes -Stiefel (HS) [11], and Polak-Ribiere (PR) [15] are given by

$$\beta_k^{FR} = \frac{\|g_{k+1}\|^2}{\|g_k\|^2} \qquad \beta_k^{HS} = \frac{g_{k+1}^T y_k}{d_k^T y_k} \qquad \beta_k^{PR} = \frac{g_{k+1}^T y_k}{\|g_k\|^2}$$

where $y_k = g_{k+1} - g_k$ and $\|.\|$denotes to $\ell_2$norm.

The line search in conjugate gradient algorithms is often based on the standared Wolfe Conditions (WC) [19]:

$$f(x_k + \alpha_k d_k) - f(x_k) \le \rho \alpha_k g_k^T d_k \ , \tag{4}$$

$$g_{k+1}^T d_k \ge \sigma g_k^T d_k , \tag{5}$$

Where d_k is a descent direction and $0 < \rho \le \sigma < 1$. However, for some conjugate gradient algorithms, a stronger version of the Wolfe line search conditions (SWC) given by (4) and

$$\left| g_{k+1}^T d_k \right| \le -\sigma g_k^T d_k , \tag{6}$$

is needed to ensure the convergence and to enhance the stability.

The form represents the pure conjugacy condition

$$d_{k+1}^T y_k = 0 \tag{7}$$

for nonlinear conjugate gradient methods. The extension of the conjugacy condition was studied by Perry [14]. He tried to accelerate the conjugate gradient method by incorporating the second-order information into it. Specifically, he used the secant condition

$$H_{k+1} y_k = s_k \tag{8}$$

of quasi-Newton methods, where a symmetric matrix H_{k+1} is an approximation to the inverse Hessian. For quasi-Newton methods, the search direction d_{k+1} can be calculated in the form

$$d_{k+1} = -H_{k+1} g_{k+1} \tag{9}$$

By (8) and (9), the relation

$$d_{k+1}^T y_k = -(H_{k+1} g_{k+1})^T y_k = -g_{k+1}^T (H_{k+1} y_k) = -g_{k+1}^T s_k$$

holds. By taking this relation into account, Perry replaced the conjugacy condition (7) by the condition

$$d_{k+1}^T y_k = -g_{k+1}^T s_k . \tag{10}$$

Dai and Liao [8] generalized the condition (10) to the following

$$d_{k+1}^T y_k = -t g_{k+1}^T s_k , \tag{11}$$

where $t \geq 0$ is a scalar. The case $t = 0$, (11) reduces to the usual conjugacy condition (7). On the other hand, the case $t = 1$, (11) becomes Perry‘s condition (10). To ensure that the search direction d_k satisfies condition (11), by substituting $d_{k+1} = -g_{k+1} + \beta_k d_k$ into (11), they had

$$-g_{k+1}^T y_k + \beta_{k+1} d_k^T y_k = -t g_{k+1}^T s_k .$$

This gives the Dai-Liao formula

$$\beta_k^{DL} = \frac{g_{k+1}^T (y_k - t s_k)}{d_k^T y_k} . \tag{12}$$

We note that the case $t = 1$ reduces to the Perry formula

$$\beta_k^{P} = \frac{g_{k+1}^T (y_k - s_k)}{d_k^T y_k} . \tag{13}$$

Furthermore, if $t = 0$, then β^{DL} reduces to the β^{HS}. The approach of Dai and Liao (DL) has been paid special attention to by many researches. In several efforts, modified secant equations have been applied to make modifications on the DL method. It is remarkable that numerical performance of the DL method is very dependent on the parameter t for which there is no any optimal choice [6].

This paper is organized as follows. In section 2 we briefly review the Three-term conjugate gradient methods. In section 3, the proposed algorithm is stated. The properties and convergent results of the new method are given in Section 4. Numerical results and one conclusion are presented in Section 5 and in Section 6, respectively.

2 Three-Term Conjugate Gradient (CG) methods

Recently many researchers have been studied three- term conjugate gradient methods. For example Narushima, Yab and Ford [13] have proposed a wider class of three term conjugate gradient methods (called 3TCG) which always satisfy the sufficient descent condition. Shanno in [17] used the well-known BFGS quasi-Newton method to obtain the following three-term CG method.

$$d_{k+1} = -g_{k+1} + \left[\frac{g_{k+1}^T y_k}{s_k^T y_k} - \left(1 + \frac{\|y_k\|^2}{s_k^T y_k}\right) \frac{g_{k+1}^T s_k}{s_k^T y_k} \right] s_k + \frac{g_{k+1}^T s_k}{s_k^T y_k} y_k \tag{14}$$

Furthermore, Liu and Xu in [12] was generalized the Perry conjugate gradient algorithm (13), the search directions were formulated as follows

$$d_{k+1}^{LX} = -g_{k+1} + \left[\frac{g_{k+1}^T y_k}{s_k^T y_k} - \left(\tau_k + \frac{\|y_k\|^2}{s_k^T y_k}\right) \frac{g_{k+1}^T s_k}{s_k^T y_k} \right] s_k + \frac{g_{k+1}^T s_k}{s_k^T y_k} y_k \tag{15}$$

where τ_k is parameter, which is Liu-Xu three-term conjugate gradient methods. When $\tau_k s_k^T y_k > 0$, the search directions defined by (15) satisfy the descent property

$$d_{k+1}^T g_{k+1} < 0$$

Or the sufficient descent property

$$d_{k+1}^T g_{k+1} \le -c_0 \|g_{k+1}\|^2, \qquad c_0 > 0 \tag{16}$$

Notice that if $\tau_k = 1$, then (15) reduces to the (14). It is remarkable that there is no any optimal choice for τ_k, However different values used for τ_k in [3], for example

$$\tau_k = 1, \quad \tau_k = c_1 \frac{y_k^T y_k}{s_k^T y_k}, \ldots$$

3 A New Three-Term Conjugate Gradient (CG) Method

The aim of this section is to derive a new three-term conjugate gradient method Aynur and Khalil (AK3 say) by using Liu-Xu (LX) method (15) and Dai - Liao (DL) CG method (3) and (12). consider the search direction given by DL

$$d_{k+1}^{DL} = -g_{k+1} + \frac{y_k^T g_{k+1}}{s_k^T y_k} s_k - t \frac{s_k^T g_{k+1}}{s_k^T y_k} s_k , \tag{17}$$

Letting $t = \dfrac{s_k^T y_k}{\|y_k\|^2}$ in equation (17) we get

$$d_{k+1} = -g_{k+1} + \frac{y_k^T g_{k+1}}{s_k^T y_k} s_k - \frac{s_k^T g_{k+1}}{\|y_k\|^2} s_k \tag{18}$$

Now equating the equations (15) and (18) i.e

$$d_{k+1} = d_{k+1}^{LX} .$$

With simple algebra and with the change signal of the last term in d_{k+1}^{LX} we get

$$\tau_k = \frac{s_k^T y_k}{\|y_k\|^2} - \frac{\|y_k\|^2}{s_k^T y_k} \tag{19}$$

Substitute (19) in the equation (15) to obtain the new search direction

$$d_{k+1}^{AK3} = -g_{k+1} + \left[\frac{g_{k+1}^T y_k}{s_k^T y_k} - \frac{g_{k+1}^T s_k}{\|y_k\|^2} \right] s_k - \frac{g_{k+1}^T s_k}{s_k^T y_k} y_k \tag{20}$$

Note that, if line search is exact i.e $g_{k+1}^T s_k = 0$ then the search direction d^{AK3} reduces to the well-known Hestenes and Stiefel β^{HS}, furthermore if $g_{k+1}^T s_k = 0$ and successive gradients are orthogonal i.e $g_{k+1}^T g_k = 0$ then d^{AK3} reduces to the CD-Fletcher method defined by $\beta_k^{CD} = -\frac{g_{k+1}^T g_{k+1}}{s_k^T g_k}$.

In the following we summarize the our AK3 algorithm.

Algorithm (AK3)

Step (1): Select a starting point $x_1 \in dom\ f$ and $\varepsilon > 0$, compute $f_1 = f(x_1)$ and $g_1 = \nabla f(x_1)$. Select some positive values for ρ and σ. Set $d_1 = -g_1$ and $k = 1$.

Step (2): Test for convergence . If $\|g_k\|_\infty \le \varepsilon$, then stop x_k is optimal ; otherwise go to Step (3).

Step (3): Determine the step length α_k , by using the Wolfe line search conditions (4)-(5).

Step (4): Update the variables as: $x_{k+1} = x_k + \alpha_k d_k$. Compute f_{k+1}, g_{k+1}, $y_k = g_{k+1} - g_k$ and $s_k = x_{k+1} - x_k$.

Step (5): Compute the search direction as: If $y_k^T s_k \ne 0$ then $d_{k+1} = d_{k+1}^{AK3}$ else $d_{k+1} = -g_{k+1}$.

Step (6): Set $k = k + 1$ and go to Step 2.

4 Convergence Analysis

In this section. We investigate the global convergence property of the algorithm (AK3). For this purpose we make the following Assumptions:

1. The level set $S = \{x \in R^n : f(x) \le f(x_0)\}$ is bounded, i.e. there exists positive constant $B > 0$ such that, for all $x \in S$, $\|x\| \le B$.

2. In a neighborhood N of S the function f is continuously differentiable and its gradient is Lipschitz continuous, i.e. there exists a constant $L > 0$ such that $\|\nabla f(x) - \nabla f(y)\| \le L\|x - y\|$, for all $x, y \in N$.

Under these assumptions on f, there exists a constant $\Gamma \ge 0$ such that $\|\nabla f(x)\| \le \Gamma$, for all $x \in S$. Observe that the assumption that the function f is bounded below is weaker than the usual assumption that the level set is bounded. Although the search directions generated by (20) are always descent directions, to ensure convergence of the algorithm we need to constrain the choice of the step length α_k. The following proposition shows that the Wolfe line search always gives a lower bound for the step length α_k. Based on the above assumptions we shall show that our method satisfies the conjugacy condition, the sufficient descent condition, and globally convergent with Wolfe line search conditions.

Theorem 1. Suppose that the step-size α_k satisfies the standard Wolfe conditions, consider the search directions d_k generated from (20) then the search directions d_{k+1} are conjugate for all k that is .

$$d_{k+1}^T y_k = -c_0 g_{k+1}^T s_k$$

Where c_0 positive constant.

Proof:

$$y_k^T d_{k+1}^{AK3} = -y_k^T g_{k+1} + \left[\frac{g_{k+1}^T y_k}{s_k^T y_k} - \frac{g_{k+1}^T s_k}{\|y_k\|^2} \right] y_k^T s_k - \frac{g_{k+1}^T s_k}{s_k^T y_k} y_k^T y_k$$

$$= -y_k^T g_{k+1} + y_k^T g_{k+1} - \frac{s_k^T y_k}{\|y_k\|^2} g_{k+1}^T s_k - \frac{g_{k+1}^T s_k}{s_k^T y_k} y_k^T y_k$$

$$= -\left(\frac{s_k^T y_k}{\|y_k\|^2} + \frac{\|y_k\|^2}{s_k^T y_k} \right) g_{k+1}^T s_k .$$

By Wolfe condition $s_k^T y_k > 0$ we have

$$\therefore \frac{s_k^T y_k}{\|y_k\|^2} + \frac{\|y_k\|^2}{s_k^T y_k} = c_0 > 0 .$$

Therefore $d_{k+1}^T y_k = -c_0 g_{k+1}^T s_k$.

Theorem 2. Suppose that the step-size α_k satisfies the standard Wolfe conditions (WC), consider the search directions d_k generated from (20) then the search directions d_{k+1} satisfies the sufficient descent condition $d_k^T g_k \le -c\|g_k\|^2$, for all k .

Proof: The proof is by induction.

If $k = 1 \Rightarrow d_1 = -g_1$, $\therefore d_1^T g_1 = -\|g_1\|^2$

know let $s_k^T g_k < -c\|g_k\|$ to proof for $k+1$, multiply (20) by g_{k+1}^T to get

$$d_{k+1}^T g_{k+1} = -\|g_{k+1}\|^2 + \left[\frac{g_{k+1}^T y_k}{s_k^T y_k} - \frac{g_{k+1}^T s_k}{\|y_k\|^2}\right] s_k^T g_{k+1} - \frac{g_{k+1}^T s_k}{s_k^T y_k} y_k^T g_{k+1}$$

$$= -\|g_{k+1}\|^2 - \frac{\left(g_{k+1}^T s_k\right)^2}{\|y_k\|^2} * \frac{\|g_{k+1}\|^2}{\|g_{k+1}\|^2}$$

$$= -\left(1 + \frac{\left(g_{k+1}^T s_k\right)^2}{\|g_{k+1}\|^2 \quad \|y_k\|^2}\right)\|g_{k+1}\|^2$$

By Couchy-Shwartiz inequality and Lipschitz condition we get

$$\frac{\left(g_{k+1}^T s_k\right)^2}{\|g_{k+1}\|^2 \quad \|y_k\|^2} \le \frac{\|g_{k+1}\|^2 \quad \|s_k\|^2}{\|g_{k+1}\|^2 \quad \|y_k\|^2} = \frac{\|s_k\|^2}{\|y_k\|^2} \le \frac{\|s_k\|^2}{L^2\|s_k\|^2} \le \frac{1}{L^2}$$

Therefore

$$d_{k+1}^T g_{k+1} = -c\,\|g_{k+1}\|^2$$

where

$$c = 1 + \frac{1}{L^2} > 0 \quad .$$

Proposition 1 ([15,16]). Suppose that d_k is a descent direction and that the gradient ∇f satisfies the Lipschitz condition for all x on the line segment connecting x_k and x_{k+1} , If the line search satisfies the Wolfe conditions (4) and (5), then

$$\alpha_k \ge \frac{(1-\sigma)\left|g_k^T d_k\right|}{L\|d_k\|^2}. \tag{21}$$

Proposition 2 ([12]). Suppose that assumptions (1) and (2) hold. Consider the algorithm (2) and (20), where d_k is a descent direction and α_k is computed by the general Wolfe line search (4) and (5). Then

$$\sum_{k=0}^{\infty} \frac{\left(g_k^T d_k\right)^2}{\|d_k\|^2} < +\infty \ . \tag{22}$$

Proposition 3 ([16]). Suppose that assumptions (1) and (2) hold, and consider any conjugate gradient algorithm (2), where d_k is a descent direction and α_k is obtained by the Strong Wolfe line search (4) and (6).If

$$\sum_{k\ge 1} \frac{1}{\|d_k\|^2} = \infty , \tag{23}$$

Then $\liminf_{k\to\infty} \|g_k\| = 0$.

For uniformly convex functions, we can prove that the norm of the direction d_{k+1} generated by (20) is bounded above. Therefore, by Proposition 3, we can prove the following result.

Theorem 3. Suppose that assumptions (1) and (2) hold, and consider the algorithm (2) and (20), where d_k is a descent direction and α_k is computed by the strong Wolfe line search (4) and (6). Suppose that f is a uniformly convex function on S, i.e. there exists a constant $\mu > 0$ such that $(\nabla f(x) - \nabla f(y))^T (x - y) \geq \mu \|x - y\|^2$ for all $x, y \in N$; then $\lim\inf_{k\to\infty} \|g_k\| = 0$.

Proof: The proof is obtained by Contradiction.

$$|\beta_k| = \left| \frac{g_{k+1}^T y_k}{s_k^T y_k} - \frac{g_{k+1}^T s_k}{\|y_k\|^2} \right| \leq \frac{|g_{k+1}^T y_k|}{|s_k^T y_k|} + \frac{|g_{k+1}^T s_k|}{\|y_k\|^2}$$

Since f is uniformly convex then $s_k^T y_k \geq \mu \|s_k\|^2$ where $\mu > 0$.

$$\therefore |\beta_k| \leq \frac{\|g_{k+1}\| \ \|y_k\|}{\mu \|s_k\|^2} + \frac{\|s_k\| \ \|g_{k+1}\|}{\|y_k\|^2}$$

By assumption (2) and Lipschitz continuity, we have $\|y_k\| \leq L \|s_k\|$ .we get

$$|\beta_k| \leq \frac{\Gamma L}{\mu \|s_k\|} + \frac{\Gamma}{L^2 \|s_k\|} = \Gamma \left(\frac{L}{\mu} + \frac{1}{L^2} \right) \frac{1}{\|s_k\|}$$

$$|\eta_k| = \left| \frac{g_{k+1}^T s_k}{s_k^T y_k} \right| = \frac{|g_{k+1}^T s_k|}{|s_k^T y_k|} \leq \frac{\|g_{k+1}\| \ \|s_k\|}{\mu \|s_k\|^2} \leq \frac{\Gamma}{\mu \|s_k\|}$$

$$\therefore \|d_{k+1}\| \leq \|g_{k+1}\| + |\beta_k| \ \|s_k\| + |\eta_k| \ \|y_k\|$$

$$\leq \Gamma + \Gamma \left(\frac{L}{\mu} + \frac{1}{L^2} \right) \frac{1}{\|s_k\|} \ \|s_k\| + \left(\frac{\Gamma}{\mu \|s_k\|} \right) \ L \|s_k\|$$

$$\leq \Gamma + \Gamma \left(\frac{L}{\mu} + \frac{1}{L^2} \right) + \frac{\Gamma L}{\mu}$$

$$\leq \Gamma \left(1 + \frac{2L}{\mu} + \frac{1}{L^2} \right)$$

$$\|d_{k+1}\| \leq \Gamma b$$

where $b = \left(1 + \frac{2L}{\mu} + \frac{1}{L^2}\right)$

$$\therefore \frac{1}{\|d_{k+1}\|} \geq \frac{1}{\Gamma b}$$

Taking the sum for both sides and considering $\|d_1\| = \|g_1\|^2 \geq \Gamma$

$$\sum_{k=0}^{\infty} \frac{1}{\|d_{k+1}\|^2} = \Gamma + \sum_{k=0}^{\infty} \frac{1}{\Gamma b} = \Gamma + \frac{1}{\Gamma b} \sum_{k=0}^{\infty} 1 = \infty$$

Contradiction we have $\lim_{k \to \infty} \inf \|g_k\| = 0$.

5 Numerical Results and Comparison

In this section, we report some numerical results obtained with an implementation of the AK3 algorithm. The code of the AK3 Algorithm is written in Fortran and compiled with f77 (default compiler settings), taken from N. Andrei web page. We selected 71 Large-scale unconstrained optimization test functions in the generalized or extended form presented in [1]. For each test function, we undertook ten numerical experiments with the number of variables increasing as n=100, 200,…, 1000. The algorithm implements the Wolfe line search conditions with $\rho = 0.0001, \ \sigma = 0.9$ and the same stopping criterion $\|g_k\|_2 \leq 10^{-6}$. In all algorithms we considered in this numerical study the maximum number of iterations is limited to 1000. The comparisons of algorithms are given in the following context. Let f_i^{ALG1} and f_i^{ALG2} be the optimal values found by ALG1 and ALG2, for problem i = 1. . . 710, respectively. We say that, in the particular problem i, the performance of ALG1 was better than the performance of ALG2 if

$$\left| f_i^{ALG1} - f_i^{ALG2} \right| < 10^{-3}$$

and the number of iterations (iter), or the number of function-gradient evaluations (fg) or the CPU time of ALG1 was less than the number of iterations, or the number of function-gradient evaluations, or the CPU time corresponding to ALG2 respectively. Figures (1), (2) and (3) shows the Dolan and Moré [5] (iterations (iter), function-gradient evaluations (fg) and CPU time) performance profile of AK3 versus DL, LX, CD and HS conjugate gradient algorithms. In a performance profile plot, the top curve corresponds to the method that solved the most problems in a(iter) or (fg) or CPU time that was within a given factor of the best((iter) or (fg) or CPU time). The percentage of the test problems for which a method is the fastest is given on the left axis of the plot. The right side of the plot gives the percentage of the test problems that were successfully solved by these algorithms, respectively. The right is a measure of the robustness of an algorithm. When comparing AK3 with the DL and LX subject (iter, fg, CPU) as in figures(1), (2) and (3) we see that AK3 is the top performer.

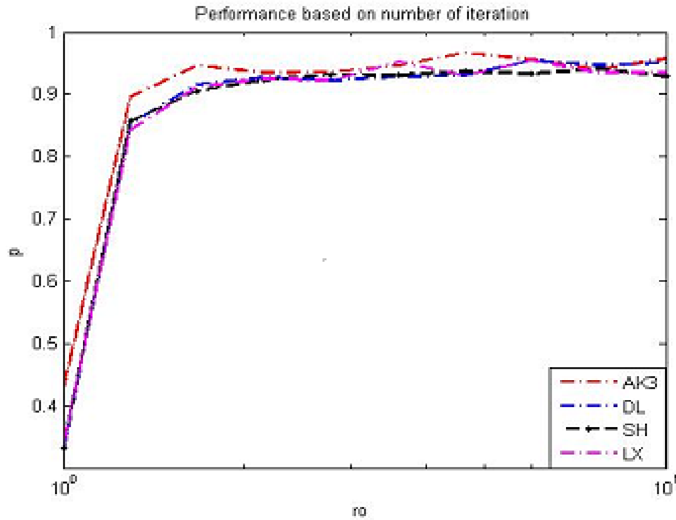

Figure 1: Performance based on number of iteration

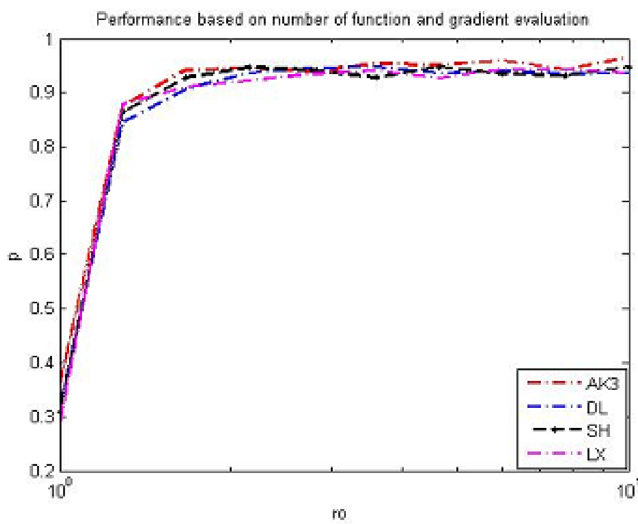

Figure 2: Performance based on number of function-gradient evaluation

6 Conclusion

In this paper, a new three –term conjugate gradient algorithm, as a modification of the DL and PS methods which generates sufficient descent and conjugate directions. Under suitable assumptions our method has been shown to converge globally. In numerical experiments, we have confirmed the effectiveness of the proposed method by using performance profile.

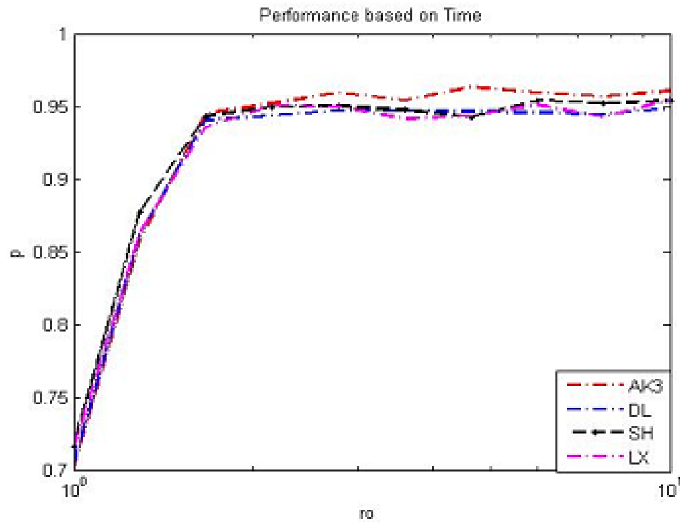

Figure 3: Performance based on time

Acknowledgment

The authors declare that this work is completely private effort and it has not been supported by any governmental, financial, educational or otherwise establishment.

Conflict of Interest Declaration

The authors declare that there is no conflict of interest statement.

Ethics Committee Approval and Informed Consent

The authors declare that declare that that there is no ethics committee approval and/or informed consent statement.

References

[1] N. Yilmaz and A. Sahiner, New global optimization method for non-smooth unconstrained continuous optimization. In: AIP Conference Proceedings. AIP Publishing LLC, 2017. p. 250002.

[2] A. Sahiner and S. A. Ibrahem, A new global optimization technique by auxiliary function method in a directional search, Optim. Lett., 13(2) 2019, 309-323.

[3] A. Sahiner, I. A. M. Abdulhamid and S. A. Ibrahem, A new filled function method with two parameters in a directional search, Journal of Multidisciplinary Modeling and Optimization, 2(1) 2019, 34-42.

[4] A. Sahiner, S. A. Ibrahem and N. Yilmaz, Increasing the Effects of Auxiliary Function by Multiple Extrema in Global Optimization. In: Numerical Solutions of Realistic Nonlinear Phenomena. Springer, Cham, 2020, 125-143.

[5] N. Andrei, An unconstrained optimization test function collection, Adv. Model. Optimization, (10) 2008, 147-161.

[6] N. Andrei, Open Problems in Nonlinear Conjugate Gradient Algorithms for Unconstrained Optimization, Bulletin of the Malaysian Mathematical Sciences Society, (34) 2011, 319–330.

[7] Y. Dai and C. Kou, A nonlinear conjugate gradient algorithm with an optimal property and an improved Wolfe line search, SIAM J. Optim., 23(1) 2013, 296-320.

[8] Y. H. Dai and L.Z. Liao, New Conjugacy Conditions and Related Nonlinear Conjugate Gradient Methods, Applied Mathematics and Optimization, Springer-Verlag, New York, 2001.

[9] E.D. Dolan and J.J. Mor´e, Benchmarking optimization software with performance profiles, Math. Programming, (91) 2002, 201-213.

[10] R. Fletcher and C.M. Reeves, Function Minimization by Conjugate Gradients. Computer Journal, (7) 1964, 149-154.

[11] M.R. Hestenes and E. Stiefel, Methods of Conjugate Gradients for Solving Linear Systems, Journal of Research of the National Bureau of Standards, 5 (49) 1952.

[12] D. Liu and G. Xu, Symmetric Perry conjugate gradient method. Comput. Optim Appl., (56) 2013.

[13] Y. Narushima, H. Yabe and J.A. Ford, A three-term conjugate gradient method with sufficient descent property for unconstrained optimization, SIAM Journal on Optimization, (21) 2013, 212-230.

[14] A. Perry, (1978). A Modified Conjugate Gradient Algorithms. Operations Research, 26, PP. 1073–1078.

[15] E. Polak and G. Ribiére, Note sur la convergence de directions conjuguée, Revue Francaise Information, (16) 1969, 35-43.

[16] M. J. D. Powell, Nonconvex Minimization Calculations and the Conjugate Gradient Method. in : Numerical Analysis (Dundee,1983), In Lecture Notes in mathematics, Springer-Verlag, Berlin, 1066, 122-141, 1984.

[17] D. F. Shanno, Conjugate gradient methods with inexact searches, Mathematics of Operations Research, (3) 1996, 244-256.

[18] W. Sun and Y. Yuan, Optimization Theory and Methods, Nonlinear programming, Springer Science, Business Media, LLC., New York, 2006.

[19] M. Wolfe, Numerical Methods For Unconstrained Optimization An Introduction, New York: Van Nostraned Reinhold, 1978.

[20] G. Zoutendijk, Nonlinear Programming, Computational Methods. Integer and Nonlinear Programming (J. Abadie ED.), North-Holland, Amsterdam, 1970.

Khalil K. Abbo, ORCID: https://orcid.org/0000-0001-5858-625X
Aynur J. Namik, ORCID: https://orcid.org/0000-0001-9100-3319